Thesis for the Degree of Master of Engineering

Automated Multistep Lateral Flow Immunoassay for the Quantification of Foodborne Bacteria Using a Smartphone Application

by
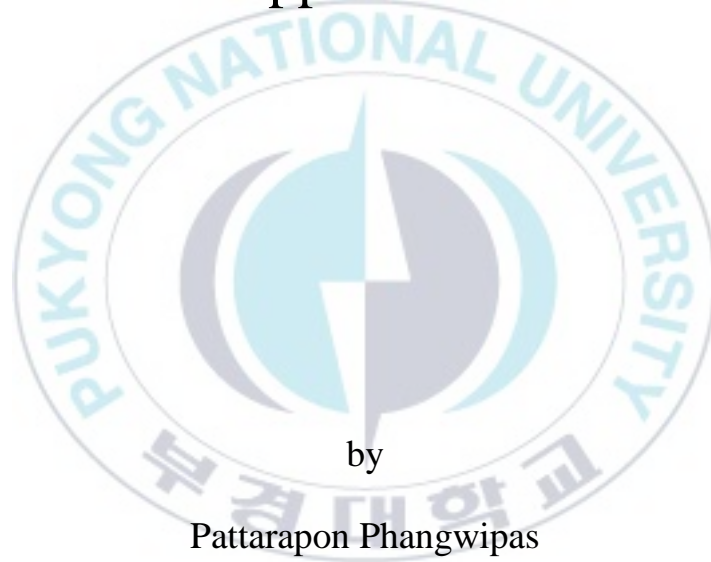
Pattarapon Phangwipas

Department of Biomedical Engineering

The Graduate School

Pukyong National University

August, 2023

Automated Multistep Lateral Flow Immunoassay for the Quantification of Foodborne Bacteria Using a Smartphone Application

스마트폰 애플리케이션을 사용한 자동화된 다중 스텝 측방유동면역분석기반의 식중독균 정량화

Advisor: Prof. Joong Ho Shin

by

Pattarapon Phangwipas

A thesis submitted in partial fulfillment of the requirements

for the degree of

Master of Engineering

in Department of Biomedical Engineering, Pukyong National University

August 2023

Automated Multistep Lateral Flow Immunoassay for the Quantification of Foodborne Bacteria Using a Smartphone Application

A dissertation

by

Pattarapon Phangwipas

Approved by:

_____

Prof Hae Gyun Lim, PhD.

(Chairman)
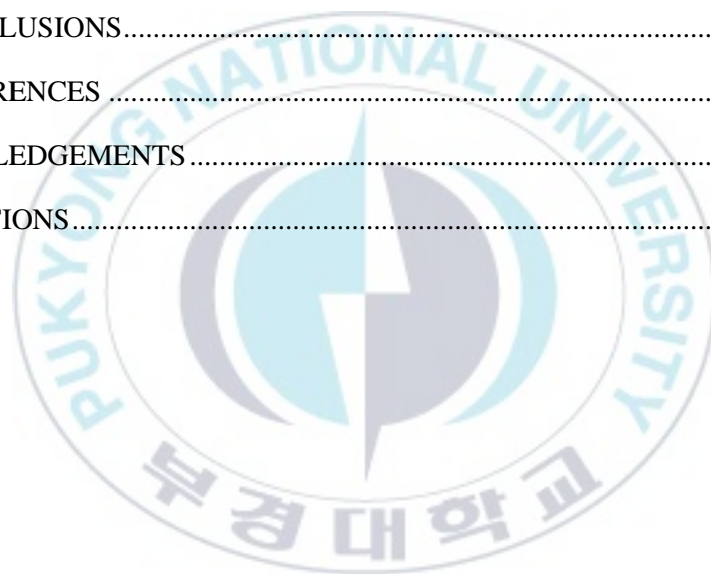
_____
Prof Sang-Hyug Park, PhD.

(Member)

_____
Prof Joong Ho Shin, PhD.

(Member)

August 18, 2023

TABLE OF CONTENTS

LIST OF ABBREVIATION

3D	Three-dimensional
a.u.	Arbitrary unit
AuNPs	Gold nanoparticles
B. cereus	*Bacillus cereus*
BSA	Bovine serum albumin
CAD	Computer-Aided Design
CFU	Colony-forming unit
CL	Control line
DAB	3,3'-diaminobenzidine
DI water	Deionized water
DNA	Deoxyribonucleic acid
ELISA	Enzyme-linked immunosorbent assay
E. coli	*Escherichia coli*
fg	Femtogram
FITC	Fluorescein isothiocyanate
FLFAs	Fluorescence lateral flow assays
h	Hour
H1N1	Influenza A virus
HAU	Hemagglutinating Unit
HRP	Horseradish peroxidase
IgG	Immunoglobulins G
LAB	Lactic Acid Bacteria
LAMP	Loop-mediated isothermal amplification
LB	Luria-Bertani
LFA	Lateral flow assay
LFIA	Lateral flow immunoassay
L. monocytogenes	*Listeria monocytogenes*

LOD	Limit of detection
mg	milligram
min	Minute
mL	milliliter
mm	millimeter
NC membrane/ NC strip	Nitrocellulose membrane/ Nitrocellulose strip
nm	Nanometer
OD	Optical density
PBS	Phosphate-buffered saline
PCR	Polymerase chain reaction
pfu/mL	Plaque-forming unit per milliliter
PMMA	Polymethyl Methacrylate
POC	Point-of-care
qPCR	Quantitative Polymerase chain reaction
S. aureus	*Staphylococcus aureus*
S. Enteritidis	*Salmonella* Enteritidis
S. Typhimurium	*Salmonella* Typhimurium
TL	Test line
V. parahaemolyticus	*Vibrio parahaemolyticus*
µL	microliter

LIST OF FIGURES

LIST OF TABLES

스마트폰 애플리케이션을 사용한 자동화된 다중 스텝 측방유동면역분석기반의 식중독균 정량화

파타라폰 펭위판

부경대학교 바이오메디컬공학과

요약

식중독은 세계에서 가장 자주 발생하는 감염성 질환 중 하나이다. 식중독 발병의 방지를 위한 방법들 중 하나로 신선한 식물의 오염을 방지하기 위한 신속한 검출 방법이 중요하다. 측방유동면역분석(LFIA)은 유해미생물 검출에 가장 사용되는 방법 중 하나로 빠르고 간단하며 저렴하고 현장 검출에 적합하지만 여전히 검출 한계가 좋지 않다는 주요 한계가 있다. 본 연구에서는 스마트폰으로 다중 스텝 측방유동면역분석 자동화로 수행하도록 설계된 회전 장치를 제어하기 위한 스마트폰 애플리케이션을 개발하고 신선한 상추에서 식중독균을 간단하게 비색 검출하는 방법을 시연한다. 블루투스 및 서보 모터를 통해 자동 회전 디바이스를 제어하는 스마트폰 애플리케이션 개발했다. 또한 스마트폰 애플리케이션의 기능을 통해 사용자는 탐지 결과를 정량화할 수 있다. 제안하는 디바이스는 두 부분으로 설계되었다. 일회용 회전 부품과 커버 박스가 있다. 오염된 상추에서 박테리아 *Escherichia coli* (*E. coli*) O157:H7 을 검출하고 회전디바이스로 정량화했다. 박테리아 검출은 30 분 동안 수행하였다. 수행한 후에 오염된 상추에서 정량화된 검출 결과는 한천 플레이트에서 콜로니를 세어 계산한 것과 유사하여 자동 회전 디바이스와 스마트폰 애플리케이션이 매우 정확함을 나타낸다. 이 디바이스는 10g 당 5×10^4 *E. coli* O157:H7 로 상추의 오염을 감지할 수 있다. 또한 특이도 검출에 대해서 다른 박테리아를 사용하였다. 본 연구의 디바이스가 높은 특이도로 수행될 수 있음을 확인한다. 이 연구는 Point-Of-Care (POC) 감지를 용이하게 하는 데 도움이 될 수 있는 자동화되고 쉽고 저렴하며 신속한 감지를 위한 디바이스를 소개한다.

Automated Multistep Lateral Flow Immunoassay for the Quantification of Foodborne Bacteria Using a Smartphone Application

Pattarapon Phangwipas

Department of Biomedical Engineering, The Graduate School,

Pukyong National University

Abstract

Foodborne disease or foodborne illness is one of the major health problems in worldwide. Thus, a rapid detection method to prevent fresh produce contamination is important to require. One of the most popularly used methods is the lateral flow immunoassay (LFIA) because it is rapid, simple, cheap, and suitable for on-site detection but still has the main limitation is the limit of detection is poor. The LFIA method can be improved by adding horseradish peroxidase (HRP) labeled antibodies. Additionally, the performance of the multistep assay is another way to improve the limitation of detection in LFIA. So, we choose this method to study in this work. In this study, we have developed a smartphone-operated device and the smartphone application for controlling the designed rotary device that automatically performs the multistep lateral flow immunoassay. This device demonstrates simple colorimetric detection of foodborne pathogens from fresh lettuce. The smartphone application was developed to control the automatic rotary device via Bluetooth and the servo motor. Additionally, the capabilities of our smartphone application allow the users to quantify the detection of pathogens. Our device was designed in 2 parts; a disposable rotary device and the cover box. The bacteria *Escherichia coli* (*E. coli*) O157:H7 from contaminated lettuce was detected and quantified by the developed rotary device within 30 min. The quantified detection result from the contaminated lettuce is similar to that calculated by counting colonies from agar plates which indicated that automatic rotary device and smartphone application are highly accurate. The device is capable of detecting contamination in lettuces as low as 5×10^4 *E. coli* O157:H7 per 10 g. Additionally, the other bacteria were used to perform the detection of specificity that we confirm that our device can be performed with high specificity. This study

introduces a device for automated, easy, low-cost, and rapid detection, which can help in facilitating Point-of-Care (POC) detection.

1. INTRODUCTION

1.1 Research Background

Foodborne disease or foodborne illness is one of the major health problems in worldwide. Approximately 600 million people get sick yearly after eating or drinking contaminated food in 2010 [1, 2]. Bacteria, viruses, and parasites, including chemical substances that enter the body through contaminated food (such as raw or undercooked meat, poultry, seafood, fresh fruits, vegetables, etc.) are the leading cause of foodborne illness [3-6]. Many researchers continue to report the outbreak of foodborne diseases in each country, such as the United States [7, 8], Canada [9], Denmark [10], France [11], and Korea [12], et al. Because the consumption of fresh produce has been increasing over the years, one of the most dominant foodborne illnesses is the outbreaks from the consumption of fresh fruit and vegetables (fresh produce) [13-15]. Although many ways of preventing a foodborne, such as keeping clean, separating raw and cooked food, cooking food thoroughly, keeping food at safe temperatures, and using pure water and raw materials [16]. Thus, a rapid detection method is required to prevent fresh produce from the contamination.

The detection method, which is the gold standard of traditional techniques for pathogen detection from fresh produce is a culture-based method [17], and the theoretical limit of detection (LOD) is 1 colony-forming unit (CFU) per portion of food sample [18]. This method involving the following process like stomaching, enrichment, bacteria culture, and the identification of target bacteria that need the long time for assay [19, 20]. First, the food sample is placed in a stomacher machine with bacteria growth media in a sterile plastic bag to remove bacteria. To enrich and increase the bacterial cells, the sample to be incubate for 18-25 h [21]. Then the enriched sample is streaked and incubated on an agar plate for colony analysis that the colonies need to be isolated to ensure purity and are incubated to be visible to the naked eye [19]. As mentioned before, the culture process requires 2-3 days for initial

results and confirmation of the specific pathogenic microorganism [22-24]. From the above, indicates that this method remains cumbersome and time-consuming.

1.2 Related Research

Due to the limitations of the culture-based method, such as a long time to analyze the results, many researchers developed several methods for rapid detection such as PCR-based methods (Polymerase chain reaction (PCR), Real-time PCR or quantitative PCR (qPCR) [25-30], Loop-mediated isothermal amplification (LAMP) [31, 32]). The PCR-based methods allow the detection of bacteria in food by detecting a specific target DNA sequence [33]. Moreover, the PCR is accurate and highly sensitive and quickly performed in 4-8 h. However, this method requires complicated PCR mix preparation, bulky instruments, and machinery fees [34]. Conventional PCR has some limitations, needs special equipment, expensive, and failed in samples with low copy numbers of the target [35]. Real-time PCR is a high-sensitivity, specificity, rapid, and reliable detection [36] but this method requires expensive detection equipment and consumables [37]. The advantage of LAMP is high sensitivity, specificity, and high predictive compared to PCR [38]. However, the LAMP needs to use a DNA polymerase which is difficult to do without an expert, requires laboratory, and has limitations for multiplexing [37].

As a more convenient alternative, an immunological-based method (immunoassay) is employed. Immunoassay is based on antibody-antigen interactions, in which antibodies bind or capture target-specific antigens [39], and enzyme-linked immunosorbent assay (ELISA) and also lateral flow immunoassay (LFIA) are widely investigated [40]. The researchers studied and demonstrated by using the detection of the ELISA process to detect pathogens in biofluids [41-46]. However, sophisticated techniques, antibody instability, and require expensive culture media, and trained technicians hinder its usage [47]. Also this method takes a long time to get results. The multiple washing steps and incubation time resulted in a long time of about 4-6 h for assay. Lateral flow immunoassay is rapid, simple, cheap, and suitable for on-site detection [39]. However, LFIA remain has main limitation that is relatively high limit

2

of detection. It's mean only detect the high concentration of bacteria. The way to improve the LFIA method is by adding chemical reagent, for example, the gold nanoparticle (AuNPs) enhancer to AuNP labels [48, 49], fluorescent dye [50-52] include chemiluminescence substrates to enzyme labels [53] such as using horseradish peroxidase labeled antibodies and luminol as a chemiluminescence substrate to effectively improve the sensitivity of the detection. Additionally, performing a multistep assay is another way to improve the limit of detection [54].

Researchers demonstrate that the ELISA was performed on LFIA to detect *Escherichia coli* (*E. coli*) O157:H7 and use a colorimetric signal in the process. This method uses a short time to analyze, inexpensive, and simple operation procedure. However, manual placement of the sample pads and absorbent pads is required. To improve this limitation, handheld devices developed using rotary-type devices were proposed [19, 55]. This device containing the multiple sample pads and absorbent pads is placed on a top layer, while the nitrocellulose (NC) test strip, which shows the result of analyzation with a test line and a control line, is placed on the bottom layer. When finishing each step of processing, the top layer is rotated 45° counterclockwise to align the subsequent pads and introduce subsequent reagents. This method demonstrates capturing and labeling the bacteria and employing a signal generation step. However, the main limitation of this method is requires manual rotation of the device and waiting during each reagent step, highlighting the need for the development of an automated detection system.

Table 1. Comparison of the related research that using the different method for detection of foodborne pathogens or bacteria.

Method	Foodborne pathogens/ bacteria detection	Limit of detection	Assay time	Reference
Real-time PCR	*V. parahaemolyticus*	10^4 CFU/mL	Not mentioned	[36]

Real-time PCR	*E. coli* O157:H7	1.69×10^2 CFU/mL	2 h	[27]
	L. monocytogenes	1.31×10^2 CFU/mL		
	S. Typhimurium	1.30×10^2 CFU/mL		
Real-time PCR	*L. monocytogenes*	599 fg for *L. monocytogenes* DNA	~2 h	[29]
	S. Typhimurium	745 fg for *S. Typhimurium* DNA		
Multiplex PCR	Lactic Acid Bacteria (LAB)	Not mentioned	2 h	[25]
mPCR-LFA	*E. coli* O157:H7	10^2 CFU/mL	100 min (1h 40 min)	[28]
mPCR-LFA LAMP	*S*. Typhimurium	10^2 CFU/mL	100 min (1h 40 min)	[28] [31]
	Giardia duodenalis	10 cysts/35 g produce	13–34 min	
LAMP	*S. aureus* *E. coli* O157:H7	10^1 CFU/mL	70 min	[32]
LAMP	influenza A (H1N1) virus	3.2×10^{-3} hemagglutinating units (HAU) per reaction	40 min	[56]
LAMP LAMP	*S. aureus*	30 CFU per reaction	40 min 45 min	[56] [57]
	E. coli O157	10 fg/μL		

Method	Target	LOD	Time	Ref
sandwich ELISA	*B. cereus*	0.9×10^3 cells/mL	3 h 25 min	[42]
sandwich ELISA	*S.* Enteritidis	5×10^4 CFU/mL	3 h 15 min	[43]
paper based ELISA	T7 phage	100 pfu/mL	3 h 16 min	[44]
paper-based ELISA	*E. coli* DH5α	1×10^5 CFU/mL	4 h	[58]
paper-based ELISA	*E. coli* DH-5α	10^5 cells/mL	<5 h	[59]
paper-based ELISA	*E. coli* O157: H7	1×10^4 CFU/mL	2 h 55 min	[45]
paper-based ELISA	*E. coli* O157: H7	1×10^4 CFU/mL	2 h 30 min	[46]
lateral flow immunoassay	*E. coli*	10^2 CFU/mL	45 min	[49]
fluorescence lateral flow assays (FLFAs)	*S. aureus*	10^2 CFU/mL	30 min	[50]
LFIA (fluorescein isothiocyanate (FITC))	*E. coli* O157: H7	10^4 CFU/mL by using a scanning reader	Not mentioned	[51]
FLFIAs	*E. coli* O157: H7	178 CFU/g in minced beef 133 CFU/mL in river water	25 min	[52]
ELISA on a lateral flow strip	*E. coli* O157:H7	10^5 CFU/mL	22 min	[19]

ELISA on a lateral flow strip	*S. aureus*	10^6 CFU/mL		
	S. Typhimurium	10^5 CFU/mL		
	B. cereus	10^5 CFU/mL	22 min	[19]
ELISA on a lateral flow strip	*E. coli* O157:H7	10^3 CFU/mL	30 min	[54]
ELISA on a lateral flow strip	*E. coli* O157:H7	5×10^4 CFU/mL	22 min	[55]

Nowadays, the smartphone is a necessity in the everyday life. The smartphone is small and suitable for a field-deployable instrument. The rapid development of smartphones has made them use of point-of-care testing such as infectious disease diagnostic, bacteria detection, virus detection, food technology, and deep learning for smartphone-based imaging devices [60, 61] including of smartphone based microscopy [62-64], lateral flow assays [65-68], paper-based microfluidic devices [69-72], and colorimetric tests [73-75] Thus, developed devices can be a potential application for detection of target analyze/ species, and analyzation. So, we use these capabilities and advantages of the smartphone to develop this work. Main advantage of smartphone for bacteria detection is faster, rapid, on-site detection, and also, increases the sensitivity of sensors.

Table 2. The developed point-of-care testing device using smartphone

Method	Function of smartphone	Reference
Smartphone-based lateral flow assay	application analysis and detection bacteria	[67]
Smartphone-based endpoint colorimetric	result recorder	[76]
isothermal LAMP-based analysis	measure the fluorescent emission from the on-chip LAMP	[77]

Paper-Based Microfluidic (colorimetric)	result recorder and analysis	[71]
smartphone-based microfluidic chip sensor	smartphone application analysis	[63]
microscopy with ultraviolet surface excitation (MUSE)	smartphone microscope, analysis	[62]
lateral flow aptamer assay	smartphone-based device was used instead of a CCD camera to read the results	[68]
lateral flow immunoassays	smartphone application analysis	[66]
paper-based microfluidic device	application, capture the fluorescence assay images, analysis	[72]
paper-based microfluidic colorimetric sensor	application, analysis	[75]
Sandwich ELISA	fluorescence detection, detector, measurement and computation	[78]
test strip based on competitive immunoassay	application, capture image and analysis	[79]

1.3 Research Purpose

In this study, we propose to develop a smartphone-operated platform device and the smartphone application for controlling the rotary device that can automate bacteria detection and analysis. We use the capabilities of the smartphone in our study to developed a smartphone-operated platform device and the smartphone application for controlling the rotary device that can automate bacteria detection and analysis. The smartphone-operated platform device consists of two parts: a disposable rotary device that can automatically rotate by using a servo motor and Arduino board were controlled by a smartphone application via Bluetooth, and the cover box that allows

stable imaging of the signal result from the test strip using a camera's phone to quantify the bacteria and prevent the ambient light. The application was used to controlled the device and analyze the result. The calibration curve and calculation the unknown signal intensity to quantify the bacteria are the function in application.

Herein, we reported the device and fabrication, perform the automate multistep lateral flow immunoassay, and demonstrate simple colorimetric detection of *E. coli* O157:H7 using the application in smartphone.

2. CONCEPTS AND THEORY

This chapter describes the concept of the device and the theory related to the work developed in this study.

2.1 Device Concept and Smartphone Application

This study demonstrates the smartphone controlled automatic device based on LFIA for detecting bacteria and analysis. The inspiration behind this device is the handheld rotary device for multistep assays [19, 55]. To develop a sensor platform that can automate and perform complicated multistep assays the rotary device has added the part of the automatic controller by using the servo motor and smartphone application.
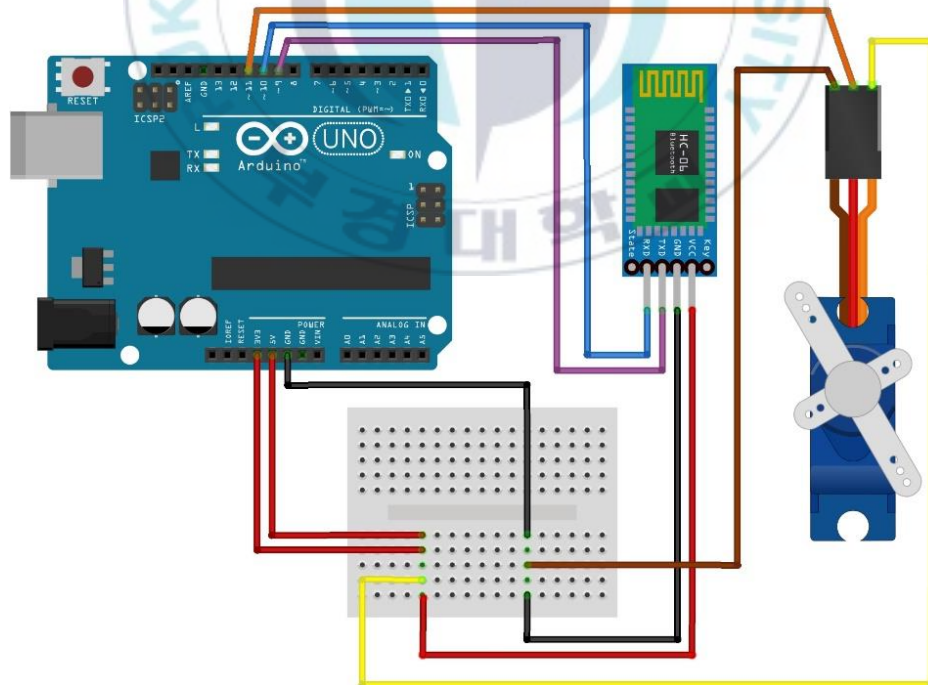
Figure 1. Schematic diagram of the electronic components used for making the automatic device.

Figure 1 shows the schematic diagram of the electronic component used in the device's operating platform. The device was operated using a smartphone application that was connected via Bluetooth. When the application operation starts, the servo motor that connects with the Arduino will be rotated. This method helps the handheld rotary device to automatically rotate.

Reagent flow direction
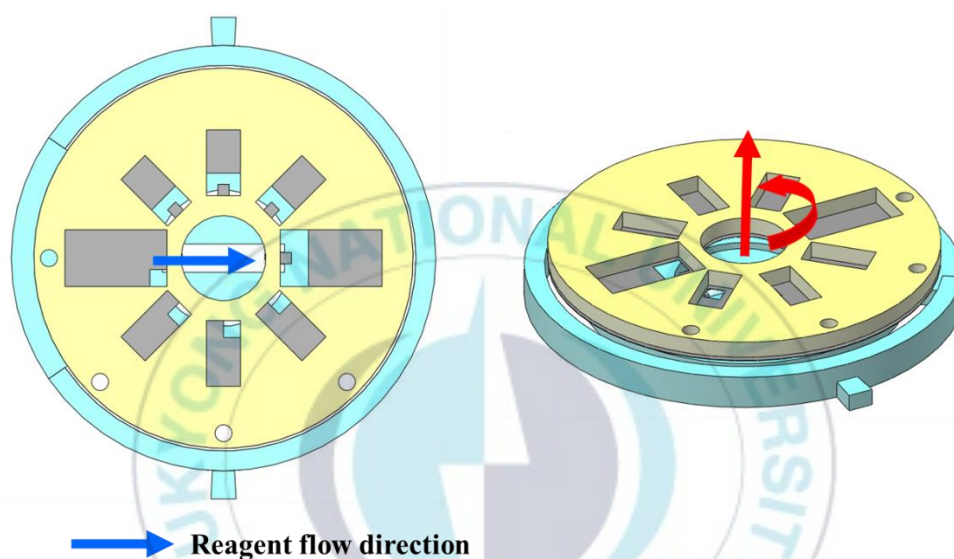
Figure 2. Direction of rotation of the rotary pad and reagent flow direction.

The rotary pad was designed to rotate counterclockwise. As shown in **Figure 2**, the reagent pad used in our study was designed in a rectangular shape with two different-sized pads: one for the sample target and the other for other reagents. The larger pad size was used for adding the sample target, while the smaller size was used for other reagents. The patterned rectangular shape was designed to ensure that the volume of the reagents fits perfectly and does not overflow. This rotary device was designed in a way that only requires pipetting once to drop the reagent and target sample into the device, and the process is automated from that point onwards.
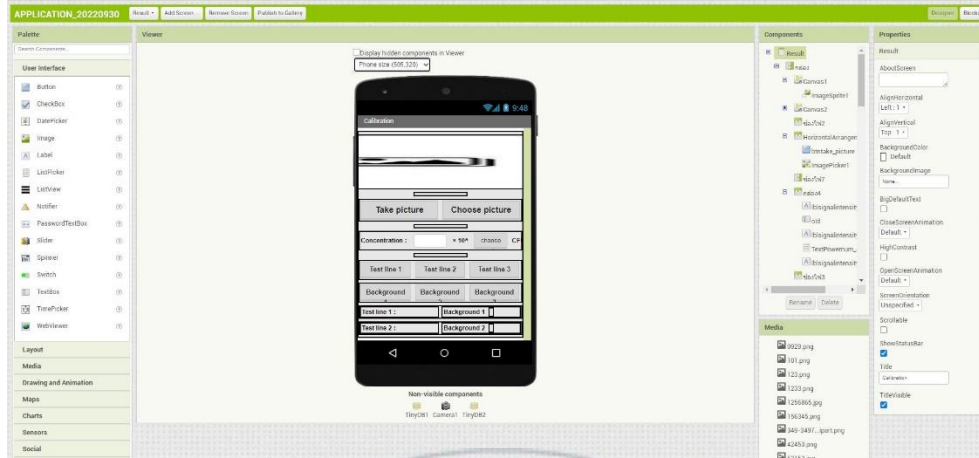
Figure 3. Screenshot of the designer editor part of MIT App Inventor.

Figure 4. Screenshot of the block editor part of MIT App Inventor.

The smartphone application used in this study is MIT App Inventor. This is an online platform that is designed to teach computational thinking concepts through developing mobile applications [80] The platform includes two main editors: the designer and the block editor, which are shown in **Figure 3** and **Figure 4**, respectively. The designer editor allows users to design the screen of the application, and drag & drop the interface. The block editor is an environment in which app inventors can visually lay out the logic of their apps.

To use the application on the smartphone, the users should utilize the connect function (**Figure 5**) and build function (**Figure 6**) of MIT App Inventor. With the

11

connect function, the users can use the application without installing it, and can edit the interface of the application at any time. On the other hand, the build function allows the application to be installed on the smartphone, but it cannot be edited. However, the users can edit the application and install it again by updating the application. In addition, users can also design application icons, as shown in **Figure 7**.

Figure 5. Screenshot of the connect function of MIT App Inventor.
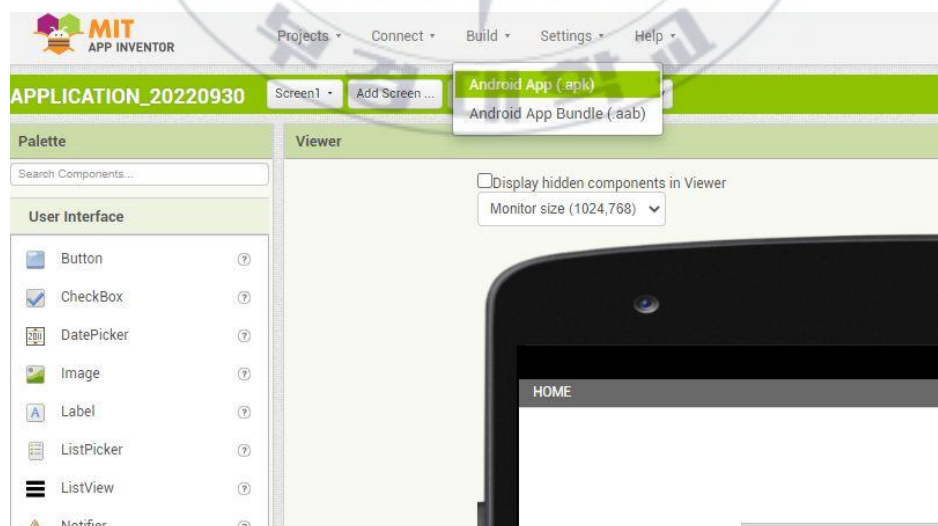
Figure 6. Screenshot of the build function of MIT App Inventor.
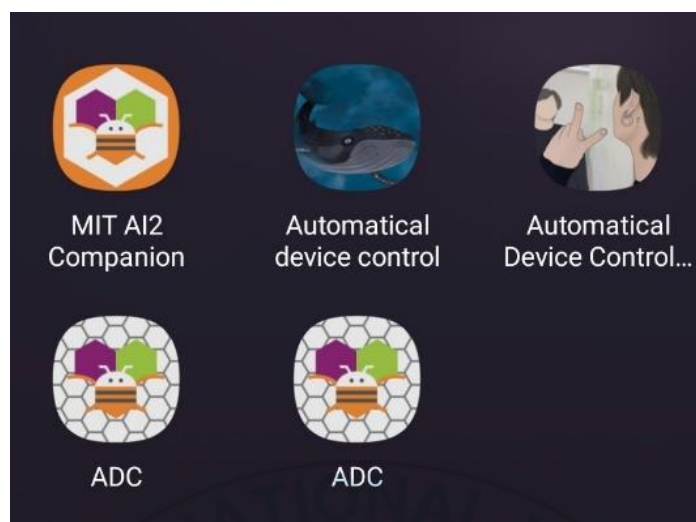
Figure 7. Screenshot of icon of application that made by MIT App Inventor.

2.2 Lateral flow immunoassay

Currently, several methods are developed for the rapid detection of POC testing including the LFIA. LFIA is an assay platform that is ideally suited for POC diagnosis [81]. According to Koczula and Gallotta [82], LFIA is a paper-based platform used for the detection and quantification of analytes in complex mixtures, In this method, the sample is placed on a test device and the results are displayed within 5–30 min. Mirica, et al also described LFIA as one of the most successful analytical methods for detecting various target molecules [83].

The standard lateral flow assay is composed of four parts, namely a sample pad, conjugation pad, membrane, and absorption pad as shown in **Figure 8**. The sample pad is the first stage of the assay that ensures the presence of the analyst in the sample and its capability to bind to the capture reagents of conjugates and on th membrane, A conjugation pad contains the conjugate labels and specific antibodies that bind to the target analyst. Commonly, Gold nanoparticles are used as a label for the process of LFIA. Additionally, enzymes have been as labels [84]. This part provides signal amplification. The Membrane or Nitrocellulose membrane allows the interaction of antibody or antigen and contains the test line and control line that displays the result of the detection. An absorption pad is the final section of lateral

flow to remove excess wastes and ensures that there is no backflow of the fluid. The reagents can flow from the sample pad to the absorption pad with the help of capillary forces.[82, 85-88]
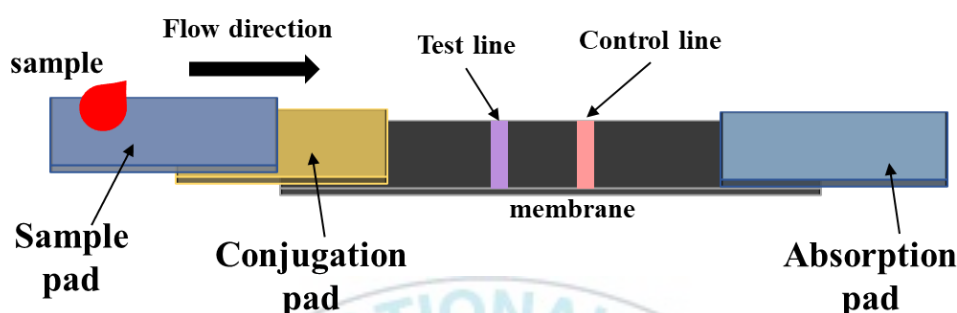
Figure 8. Schematic representation of a typical LFA strip.

In a standard lateral flow assay, if the sample contains the target analyst, it will bind to the capture reagents on the conjugate pad and form a complex. This complex then migrates along the membrane, and if the target analyst is present, it will bind to the capture reagents on the test line, resulting in a visible signal. The lines appearing at different intensities could be interpreted through naked eyes of a dedicated reader, as shown in **Figure 9**. The control line confirms that the assay is working correctly by detecting the presence of the control reagents on the membrane. If both the test line and control line appear, it indicates a positive result. If only the control line appears, it indicates a negative result. The intensity of the signal on the test line can vary, depending on the amount of target analyst present in the sample. The results can be interpreted visually without the need for specialized equipment.

Test line   Control line

Positive detection

Negative detection

Invalid detection

Invalid detection
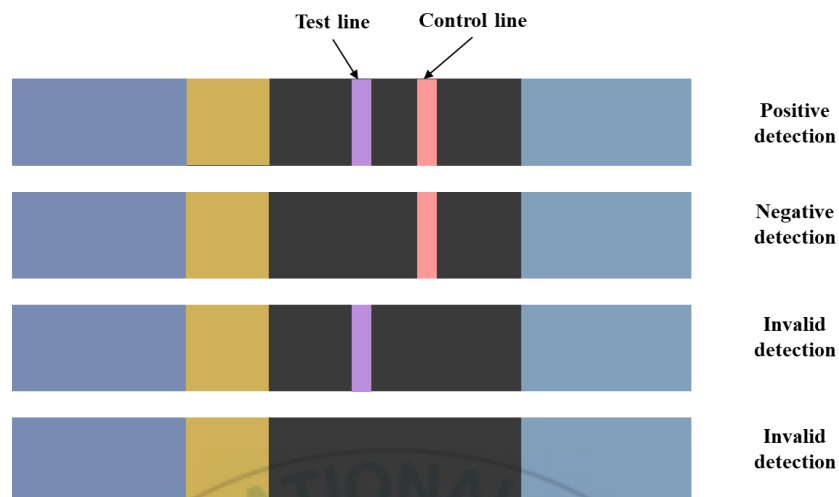
Figure 9. The schematic representation of test result obtained from LFIA strip.

Type of lateral flow immunoassay currently there are 2 types; sandwich format and competitive format, as shown in **Figure 10**. The sandwich format is used for the detection of large analysts. The result in which the signal intensity is proportional to the amount of analyst present in the sample. A Competitive format is used for the small analysts. In this format, only the control line appears to indicate that the result is positive [86, 89, 90].
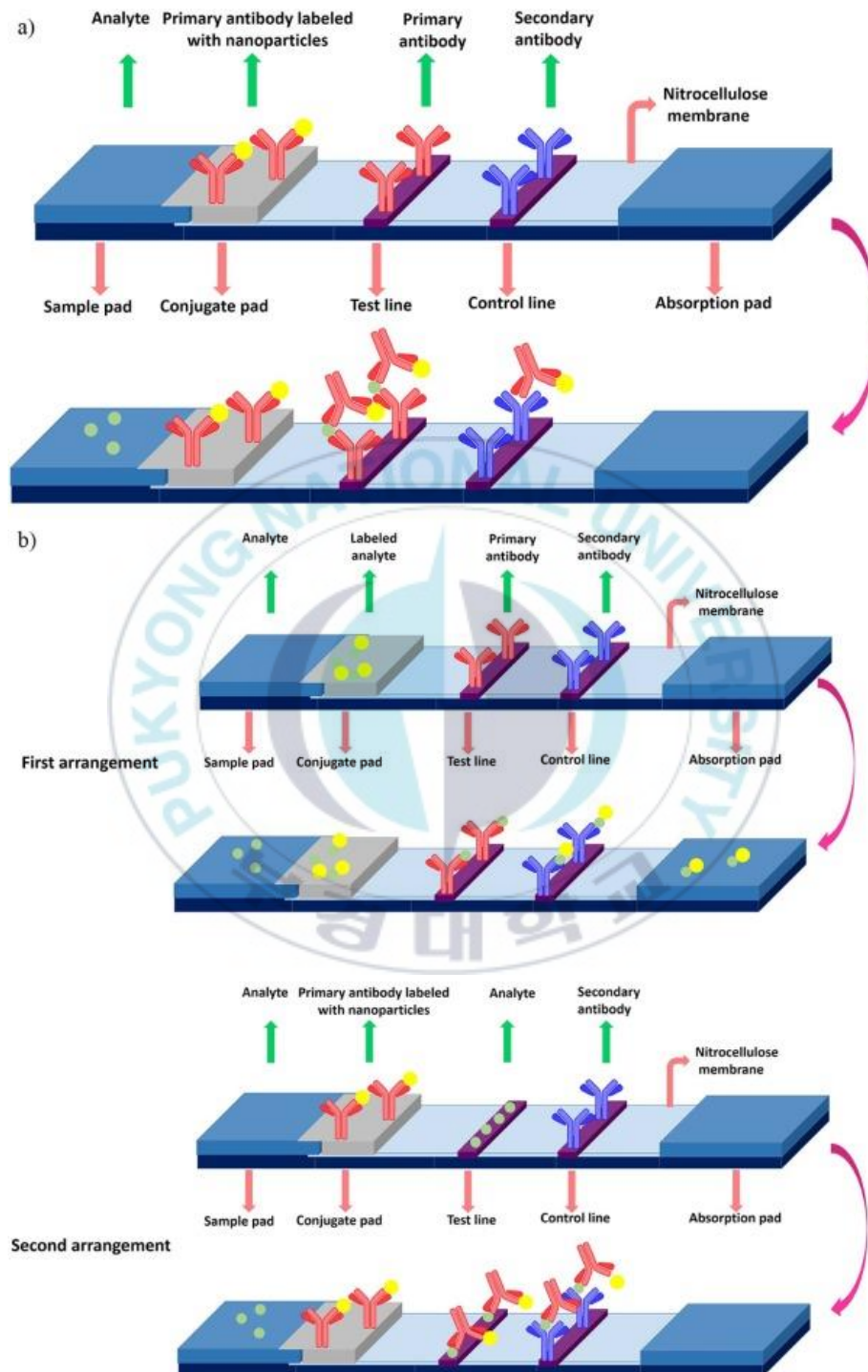
Figure 10. (a) sandwich format lateral flow assay. (b) competitive format lateral flow assay (adopted from Reference. [91]).

There are several advantages of using LFIA in diagnosis field including fast responses, low cost, simple test procedure, easily scalable, low sample volume required, and user-friendly operation [82]. However, in the LFIA there is a limitation in sensitivity, accuracy of the test relies on the quality, and additional equipment may be necessary [85].

2.3 Horseradish peroxidase for Enzyme-Labeled Conjugates in LFIA

Horseradish peroxidase (HRP) is a glycoprotein and belongs to a large class of peroxidases [92, 93], and is commonly used as enzyme label [94]. HRP is useful for fluorescence microscopy, ELISA, and Immunoassay [95]. It is often used to label nanoparticles and amplify signal detection [96] in assays by catalyzing the conversion of a chromogenic substrate, such as 3,3',5,5'-Tetramethylbenzidine (TMB), 2,2'-Azinobis [3-ethylbenzothiazoline-6-sulfonic acid] (ABTS), o-phenylenediamine dihydrochloride (OPD), and 3,3'-Diaminobenzidine (DAB) to detect the target [97, 98]. HRP-labeled antibody conjugates have been used to detect Rabbit IgG [99]. In LFIA, HRP is used as the label in a conjugate pad. And also used as the detection reagent because of its stability, and the availability of a wide range of colorimetric substrate [100]. HRP has a smaller size and a higher turnover rate compared to AuNPs, which are commonly used for colorimetric labeling and signal amplification in conventional LFIA. In the comparison of the AuNPs-based immunoassay and HRP-based immunoassay, the limit of detection by using HRP as labels is lower than by using AuNPs as labels [101]. Additionally, HRP is small in size and the molecular weight of HRP is 40,000 [102] which decreases the probability of interference with the conjugated protein function, also the HRP has a high turnover rate [100].

2.4 DAB staining

3,3'-Diaminobenzidine (DAB) is an organic compound with the formula $(C_6H_3(NH_2)_2)_2$ [103]. DAB is oxidized in the presence of *Horseradish peroxidase* and hydrogen peroxide (H_2O_2) resulting in the generation of a brown color [103, 104].

An advantage of DAB chromogenic (colored precipitate formed during the reaction between HRP and DAB) staining is not light sensitive and stored for many years [103].
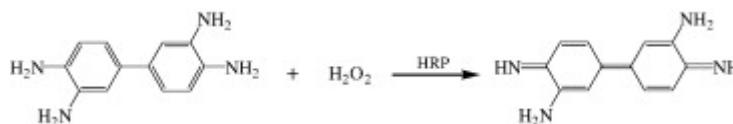
Figure 11. The process of the HRP-catalyzed oxidation reaction of DAB by H_2O_2 (adopted from Reference. [105]).

3. MATERIAL AND EXPERIMENTAL

This chapter describes the materials and experimental parts to obtain the results of the study including materials and reagents, Bacteria preparation, Design and Fabrication of the device, Application development, Principle of Performing Automated Multistep LFIA, Preparation of bacteria target for Detection of Bacteria from Contaminated Lettuce, Detection of Specificity, and Sensor Stability.

3.1 Materials and reagents

A total of 1 mg/mL of goat anti-rabbit IgG (R5506; Sigma-Aldrich, St. Louis, MO, USA) and 1 mg/mL of mouse *E. coli* O157 antibody (MBS568193; My BioSource, San Diego, CA, USA) was dispensed as the control line the test line on the NC membrane (NCPF-SN12, mdi Membrane Technologies, Inc., Camp Hill, PA, USA), respectively, and then allowed to dry at room temperature (RT). Horseradish peroxidase (HRP)-conjugated anti-*E. coli* IgG (ab20425; Abcam, Cambridge, UK) was diluted to 10 ng/mL in Phosphate-buffered saline (PBS) containing 3% bovine serum albumin (BSA) and 0.05% Tween-20 and used as a labeling agent. Wash buffer was prepared with PBS containing 3% BSA and 0.05% Tween-20. Preparation of the 3,3′-diaminobenzidine (DAB) (D4293; Sigma-Aldrich Korea, Seoul, Republic of Korea) solution can be done by dissolving and mixing in 5 mL of deionized water (DI water) by using Vortex-Genie 2 (Scientific Industries, Bohemia, NY, USA) to use this solution as a substrate. *E. coli* O157:H7 (ATCC 35150) was used as a bacteria target. *S. aureus* (ATCC 12600), and *S.* Typhimurium (ATCC 14028) were used to observe the detection specificity test. In addition, 1 mg/mL goat anti-rabbit IgG containing 1% trehalose and 1 mg/mL mouse *E. coli* O157 antibody containing 1% trehalose were dispensed onto an NC membrane. The NC membrane with immobilized antibodies was stored at 4 °C in a box to prevent exposure to light. This was prepared for the strip stability test.

3.2 Bacteria preparation

For the experiment of bacteria detection, we used the *E. coli* O157:H7 as the target bacteria. *E. coli* O157:H7 was cultured in 5 mL Luria Bertani (LB) broth and shaken at 200 rpm in a shaking incubator (SHI1; Labtron, Seoul, Republic of Korea) overnight. The optical density (OD) was measured at a wavelength of 600 nm using the Epoch ™ Microplate Spectrophotometer and was calculated to quantify the concentration of bacteria based on the growth curve. The cultured bacteria were diluted by 2% BSA in PBS to $5\times10^0 - 5\times10^7$ CFU/mL. For the experiment of specificity detection, we used *E. coli* O157:H7*, S. aureus*, and *S.* Typhimurium for this experiment. After the bacteria were cultured, measured the OD and calculated to find the concentration as same as the above, the three different bacteria were diluted by 2% BSA in PBS to 5×10^7 CFU/mL.

3.3 Design and fabrication of the device

The device was divided into two main parts: the operating platform (electronics) and the disposable rotary devices, as shown in **Figure 12**. The operating platform was designed in CAD file using SOLIDWORKS software and printed using the Sindoh 3D Printer (3DWOX 1, Sindoh, Republic of Korea). This part consists of the operating platform box (electronics box) and the cover box. Inside the operating platform box contains a Bluetooth (HC-06 Bluetooth Module, P0000PKG; Anyang, Republic of Korea), Arduino board, and servo motor that allows the device to rotate, as shown in **Figure 1**. The cover box was designed like a dark room to be responsible for preventing variations in ambient light during capturing the resulting image. To position the smartphone in the same place when during the experiment, a jig is included in the cover box (**Figure 13**). The rotary parts consist of the bottom piece and the top piece, which are made from 3 mm thick poly methyl methacrylate (PMMA) plates, and were patterned and etched by using a laser cutter (KL-900L; KISON, Seongnam, Republic of Korea). The top piece is the rotating part and the bottom part was fixed with the electronic box.
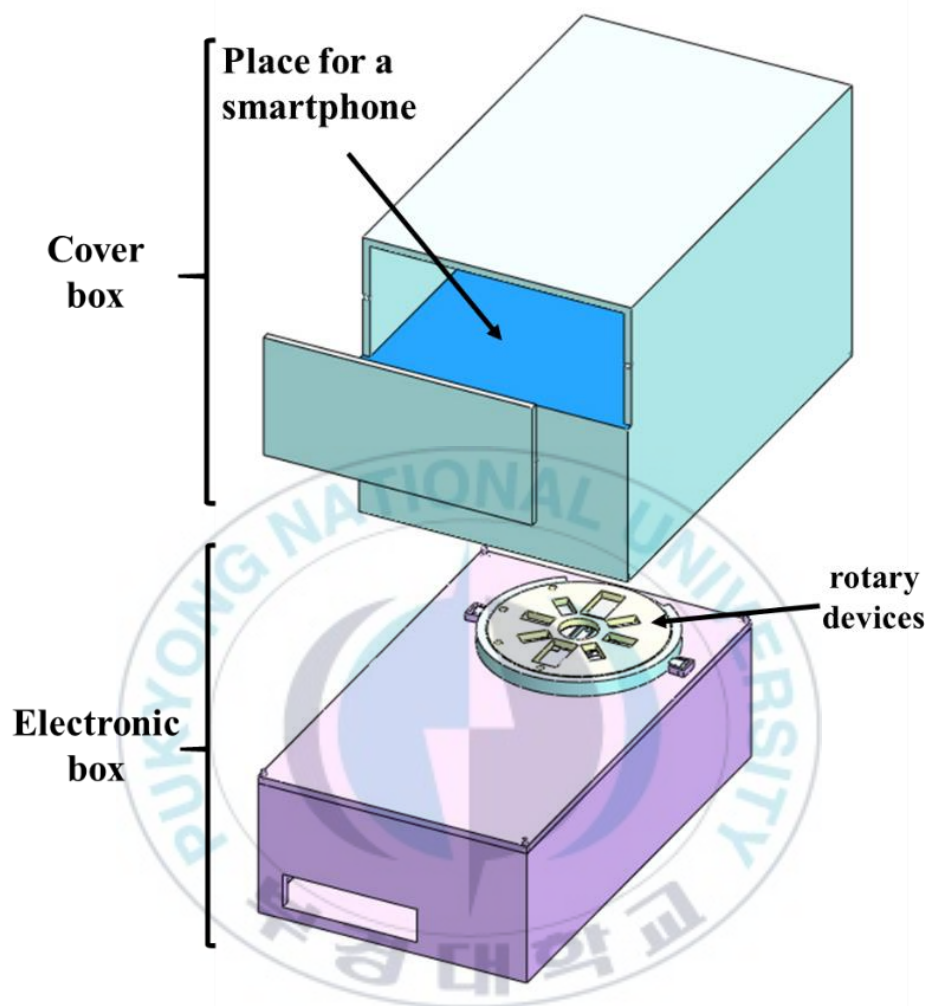
Figure 12. Schematic of the operating platform and the disposable rotary devices showing the cover box and the electronic box with the rotary device placed inside.
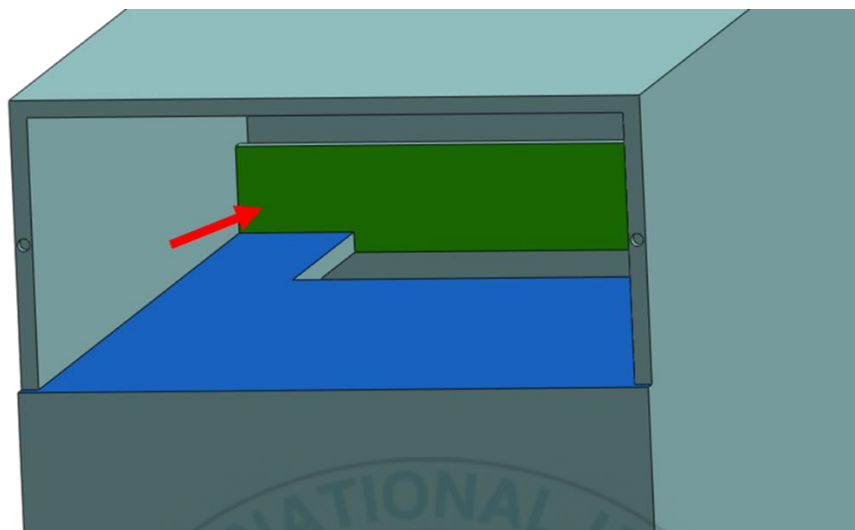
Figure 13. A jigs inside the cover box to position the smartphone.

The diameter of the rotary pad (top piece) was 67 mm, which contains eight channels for 4 sample pads and 4 absorbent pads, as shown in **Figure 14a**. The through-holes were patterned on the OHP Transparency film with a laser cutter and attached to the top piece with double-sided tape to fix the sample pads and absorbent pads with the channels, and prevent falling, as shown in **Figure 14b**. The center of the bottom piece was placed with the NC strip. To fix the NC strip on the bottom piece, the NC strip holder was patterned and cut on the OHP film, and attached to the bottom piece, and then the NC strip was inserted under the NC strip. The top piece has four circular holes, which are used for fixing the prongs and connected to the servo motor. The bottom piece has an arc-shaped cut-out. Therefore, the top piece can be rotated by the servo motor without rotating the bottom piece, which is fixed by the key slots, as shown in **Figure 15**. The servo motor rotates and then the prongs will rotate together the top piece, waits for a specified duration for reagent flow, and then rotates again to introduce a subsequent reagent to the NC strip. The series of rotation movements -and- waiting allows the user to perform an automated multistep assay on the LFIA strip.
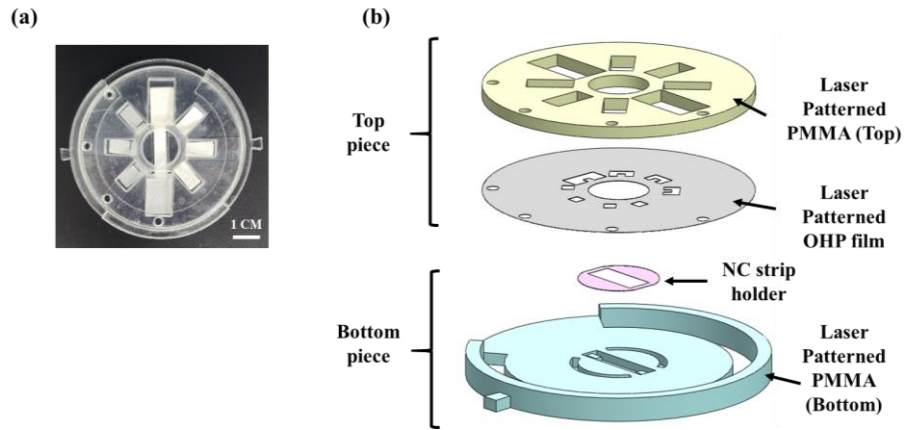
Figure 14. The rotary device (a) Photo of the rotary device with the NC membrane, glass fiber pads, and absorbent pads installed in it. (b) Exploded view of the rotary device showing each layer and its components.
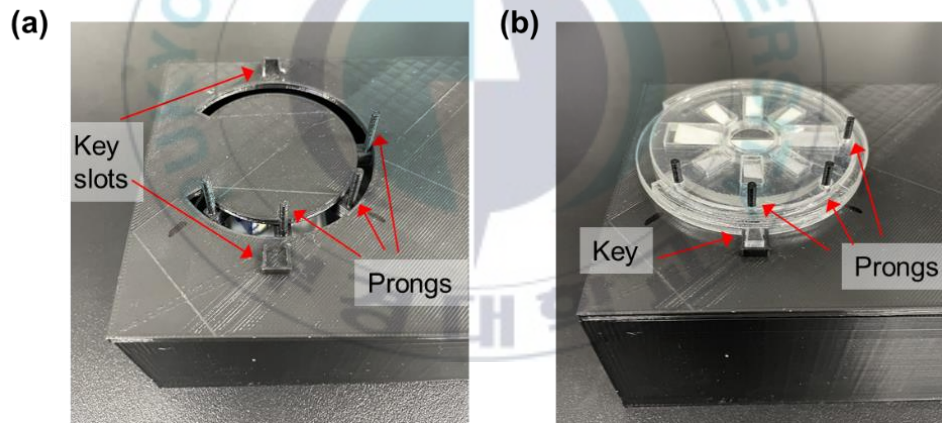
Figure 15. Photo of the operating platform showing the assembly of the electronic box (a) without the rotary device. Red arrows show the location of the key slots and prongs. (b) with the rotary device. The key is placed into the key slot to fix the bottom piece and the prongs penetrate the four holes of the top piece so that the servo motor can rotate the top piece only.

3.4 Application Development

The application was developed using the MIT App Inventor and operates by using the Samsung Galaxy S20 +5G (Samsung, Republic of Korea), which consists of 3 functions: Setting and Run, Calibration, and Calculation, as shown in **Figure 16**.
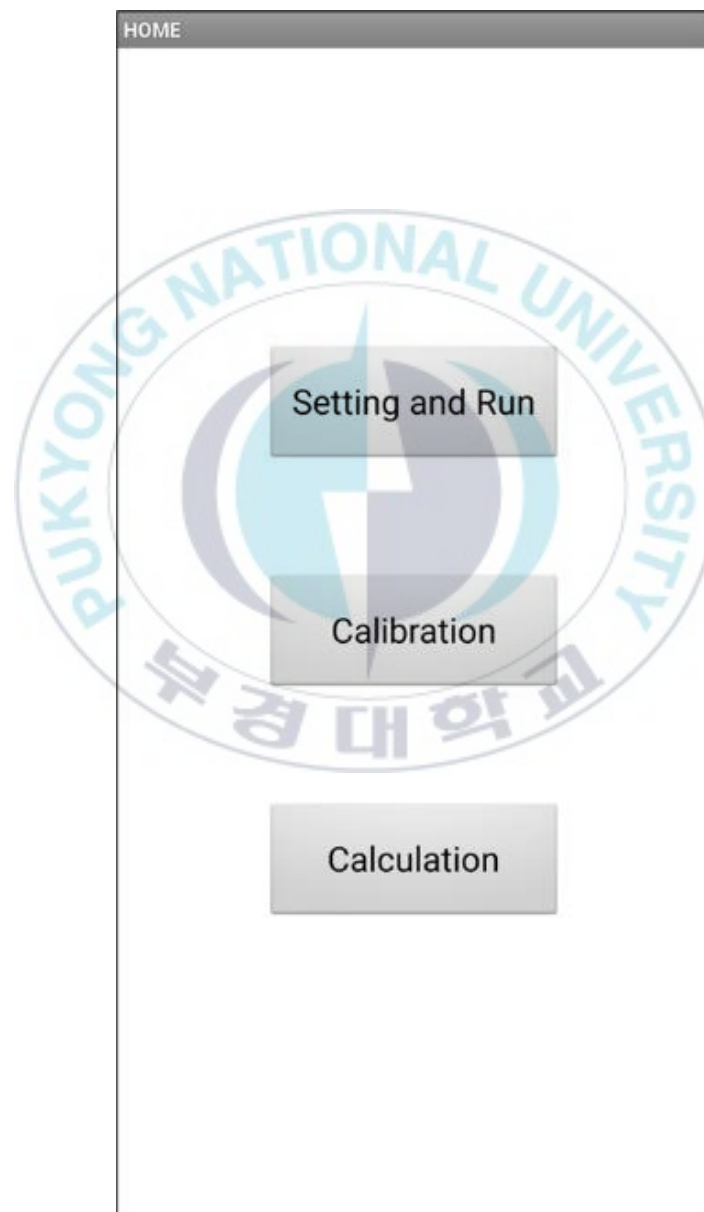
Figure 16. Screenshot of the first page of the application; the user can select the Setting and Run, Calibration, and Calculation menus.

Figure 17. Screenshot of the Setting and Run, which is a page used for inputting flow durations.

The first function is Setting and Run, as shown in **Figure 17**. On this screen, the user can connect the application to the device via Bluetooth. The assay starts with the user setting the duration for the assay step. In this study, we used 10, 5, 5, and 10 min for the assay step sequence, and the timer begins counting down upon clicking

the Start button. During the countdown, the reagents are delivered from the sample pad to the absorbent pad via capillary force. The device is automatically rotated 45° counterclockwise to the next step of the assay when the set time or the countdown timer reaches zero. When the last step assay is finished (countdown timer reaches zero), the smartphone application will capture the NC strip in the second function. Additionally, this screen also has the Stop button and Reset button to stop and reset the operation of the device, respectively. When the Stop button was clicked, the device will stop, and when the Reset button was clicked, the device will return to the initial position and the number of countdown timers was set to zero.

Figure 18. Screenshots of the first page of the Calibration screen, show the image of the NC strip, and the user can specify the known concentration.
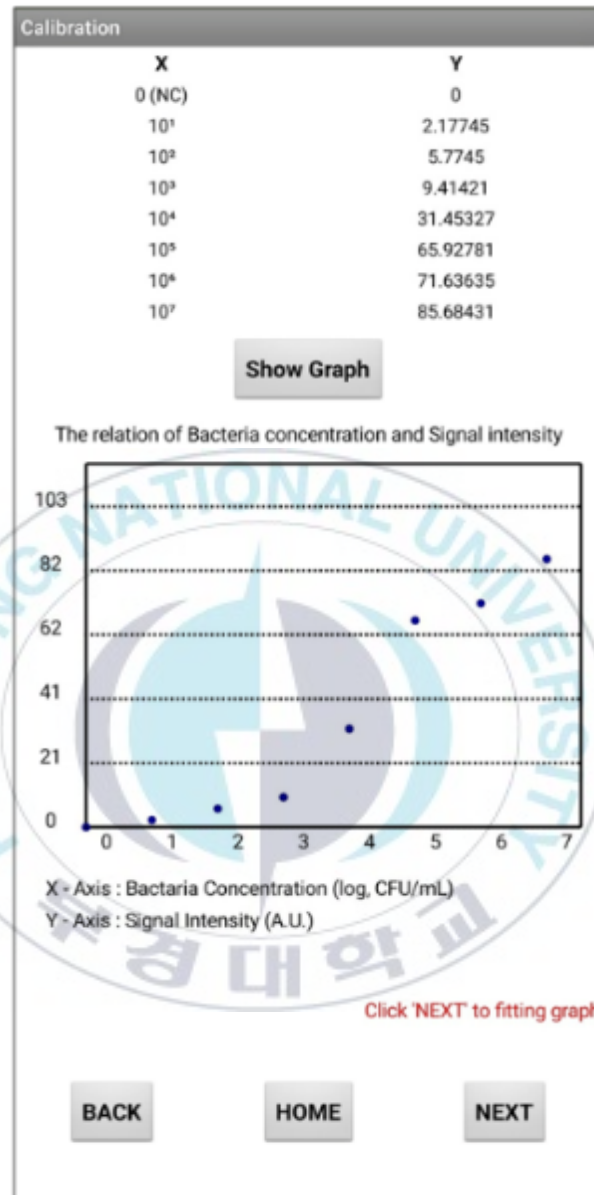
Figure 19. Screenshots of the second page of the Calibration screen, show the Calibration curve.
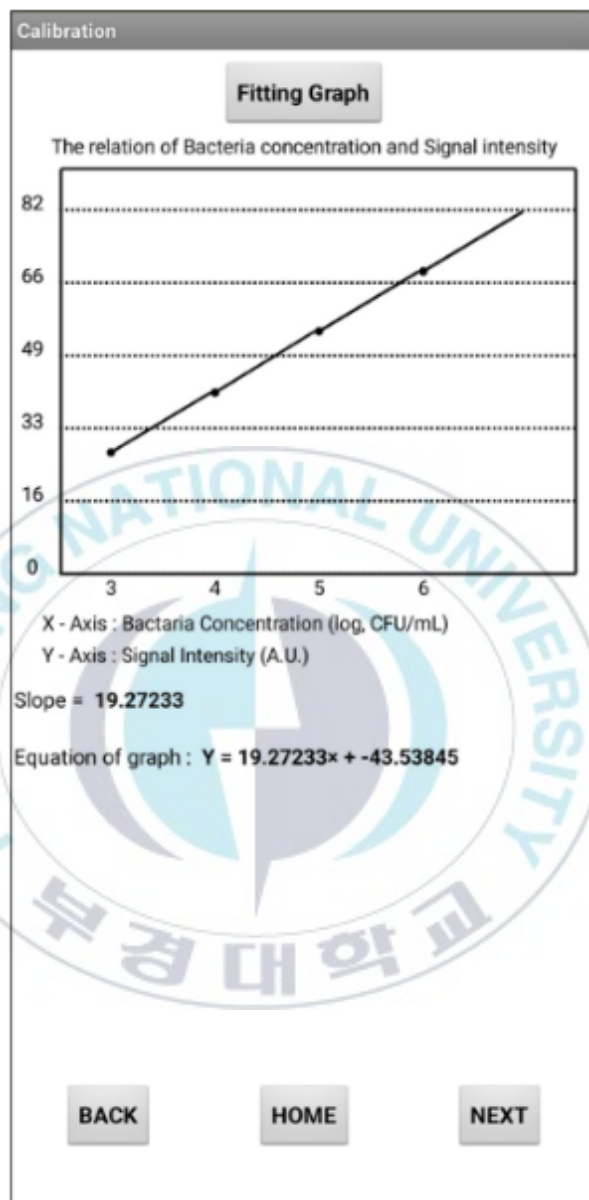
Figure 20. Screenshots of the last page of the Calibration screen, show a
Linear fit curve that shows the slope and the equation of the curve.

The second function is Calibration, which is used to make a calibration curve
from known bacteria concentrations. In this study, we used the bacteria *E. coli*
O157:H7 with a concentration ranging from 5×10^0 to 5×10^7 CFU/mL for
performing the automated multistep LFIA. After the result or a signal from the test

line appears on the NC membrane (countdown timer reaches zero in the function of Setting and Run), its image of the result is captured using the smartphone by clicking the Take picture button, as shown in **Figure 18**. On this screen, we selected the area of the test line to quantify the signal intensity. The Get the values button was clicked to store the values of each bacteria target. Additionally, this screen also has the Choose picture button, which the user can insert the resulting image from the smartphone's galleries to quantify the signal intensity. The values of signal intensity of each sample target were used to make the calibration curve based on a regression equation, as shown in **Figure 19** and **Figure 20**, in which **Figure 21** shows the values of signal intensity received from the first page of this function and was used to make the curve, and **Figure 20** shows the linear fitting curve of the relation between bacteria concentration and signal intensity.

Lastly, the Calculation function is shown in **Figure 21**. This function was used to calculate the concentration of bacteria in a liquid sample that we called the unknown sample based on the calibration curve from the Calibration function. When the signal from the unknown sample, which is the intensity of the signal on the test line of the NC membrane is quantified and input into the application, the user can calculate an estimated bacterial concentration based on the calibration curve.
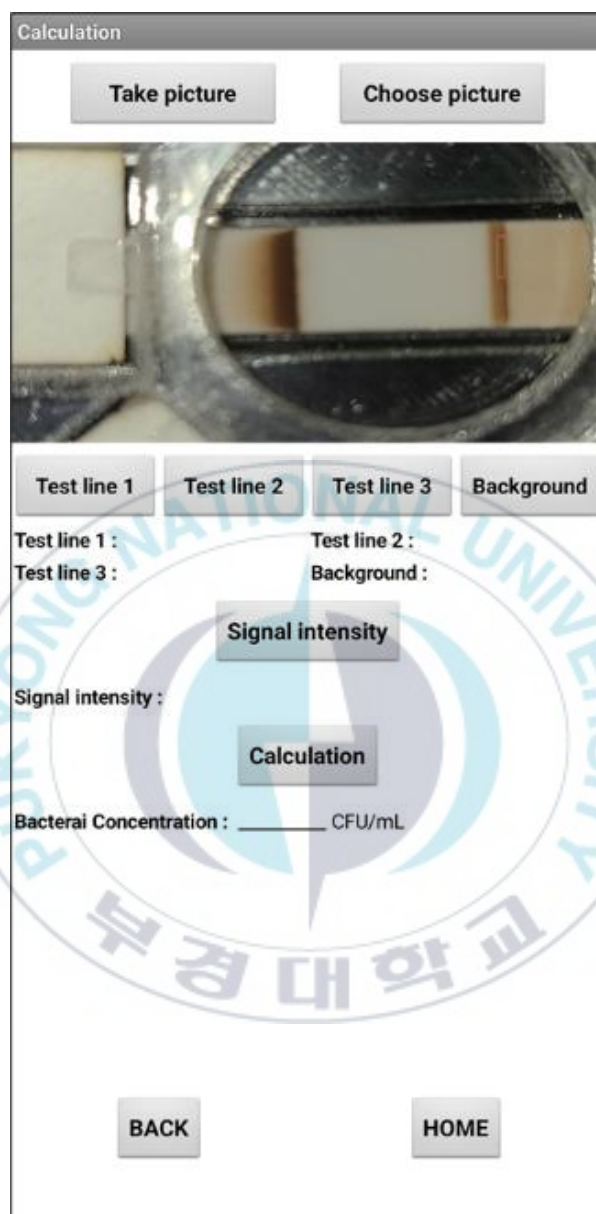
Figure 21. Screenshot of the Calculation, showing the image of the test result of an unknown sample, and the calculated bacteria concentration based on the calibration curve.

3.5 Principle of Performing Automated Multistep LFIA

As shown in **Figure 22a**, the rotary pad consists of four sample pad channels. The first sample pad (S1) was designed to contain 90 µL of the sample for bacteria capturing assay step, and the other sample pads (S2–S4) were designed to contain 40 µL of the assay reagents for labeling, washing, and signal generation step respectively.

Before loading the sample into S1, S2 was loaded with HRP-conjugated anti-*E. coli* IgG, wash buffer was loaded into S3, and prepared DAB solution was loaded into S4. The assay commenced by loading 90 µL of *E. coli* O157:H7 suspended in 2% BSA into S1, then allowing the sample to flow for 10 min. While the sample containing the bacteria is delivered through the NC membrane, the target bacteria are captured by the antibodies immobilized at the test line, as shown in **Figure 22b**. After 10 min of sample flow, the rotary device (top piece) automatically rotates 45° counterclockwise to deliver HRP-conjugated anti-*E. coli* IgG, which was in S2. In this step, the HRP-conjugated anti-*E. coli* IgG binds with the captured bacteria at the test line and anti-rabbit IgG at the control line is shown in **Figure 22c**. After 5 min of the HRP-conjugated anti-*E. coli* IgG flow, the rotary device automatically rotates to deliver the wash buffer for 5 min to eliminate non-specific bacteria from the NC membrane, as shown in **Figure 22d**. Lastly, after finishing the washing step, the rotary pad rotates again to perform the last step. In the last step, the DAB solution flows through the NC membrane to generate the signal for 10 min. The DAB is oxidized by hydrogen peroxide to change the color to brown, which allows the signal to be appeared on the NC membrane, as shown in **Figure 22e**. The assay can be automatically finished in 30 min using the smartphone application and the device. The advantage of this method is required pipetting only one time for loading the sample and reagent, after that the device will do the assay automatically.
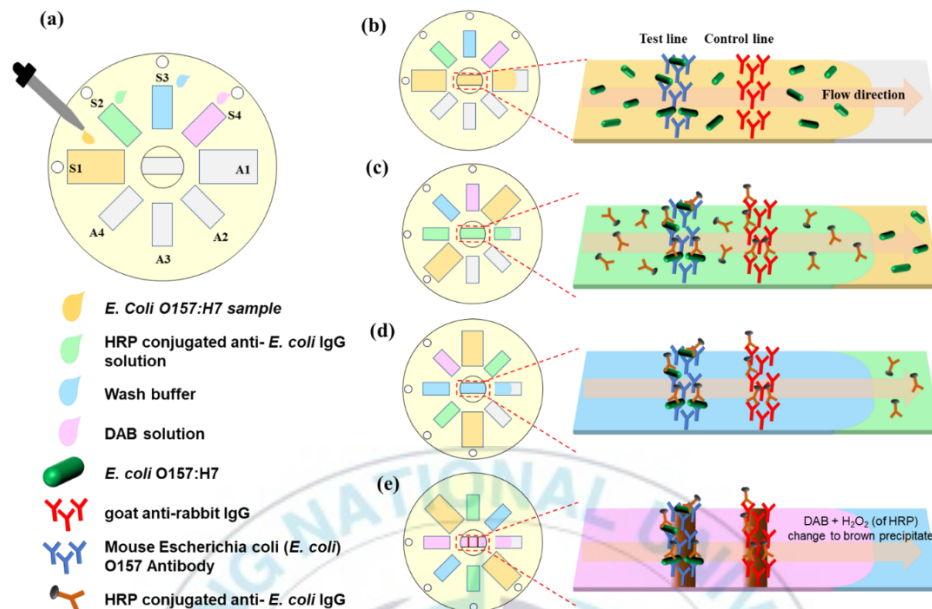
Figure 22. Schematics of each step of strip-based multistep immunoassay showing (a) loading the reagent for assay on the rotary pad, (b) bacteria capturing step, (c) HRP-IgG labeling step, (d) washing step, and (e) signal generation was using DAB steps.
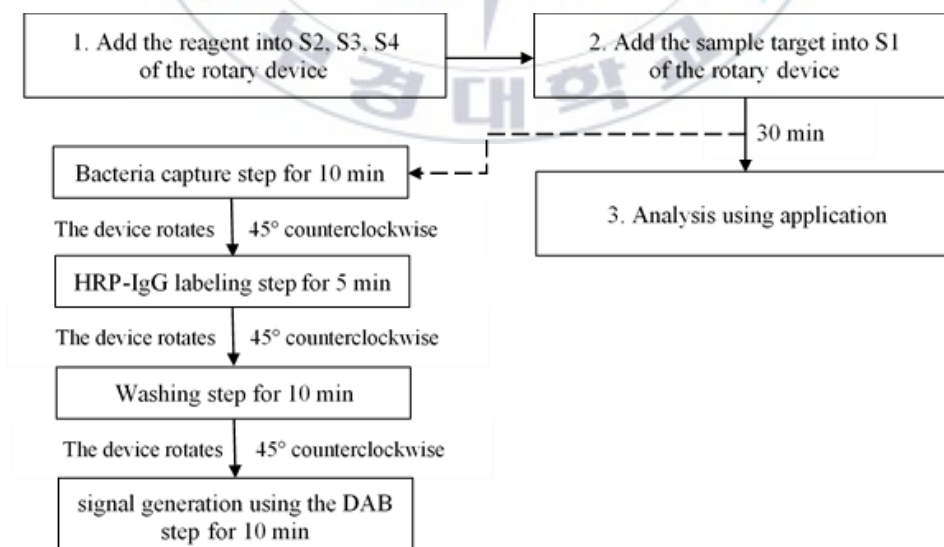
Figure 23. Diagram of performing Automated Multistep LFIA.

3.6 Preparation of bacteria target for Detection of Bacteria from Contaminated Lettuce

To support our device can actually be used to detect bacteria from fresh vegetables. *E. coli* O157:H7 was incubated in the shaking incubator overnight, and then the optical density (OD) of the bacteria was measured using a spectrophotometer and a growth curve to quantify the concentration, which was then diluted to 5×10^7 CFU/mL by adding PBS. The solution containing the bacteria was centrifuged at $3000 \times g$ (gravity) for 20 min, and the bacteria were re-suspended in PBS. Then, the bacteria were further diluted to the target bacteria concentrations of 5×10^4, 5×10^5, and 5×10^6 CFU/mL. In total, 10 µL of each solution containing bacteria were log-diluted and dotted on an agar plate to measure the actual concentration, the experiment was done in the CleanBench to prevent danger from used bacteria. The colonies on agar plates were counted in the next day to compare with the LFIA result. A total of 100 µL of each bacteria target was dropped onto the lettuces at different spots and allowed to dry for 5 min before being placed in a plastic bag. The 45 mL volume of PBS was poured into each plastic bag with lettuce. Then, the bags were shaken for 2–3 min to retrieve the bacteria from the lettuce. The solution from the plastic bag was poured into two 50 mL conical tubes and centrifuged at $3000 \times g$ for 20 min. After removing the supernatants, the samples (the infranatant) were re-suspended in 300 µL of PBS in a micro-centrifuge tube. A portion of the sample was mixed with BSA to reach the final concentration of 2% BSA. A 90 µL volume of the sample was loaded into the device for the detection.

3.7 Detection of Specificity

Herein, *E. coli* O157:H7, *S. aureus*, and *S.* Typhimurium were used as the sample. The concentration of the target bacteria is 5×10^7 CFU/mL of each sample. This experiment was performed by automated multistep LFIA with our device and application. The result of three different target bacteria was compared with the negative control result that used 2% BSA in PBS as the sample.
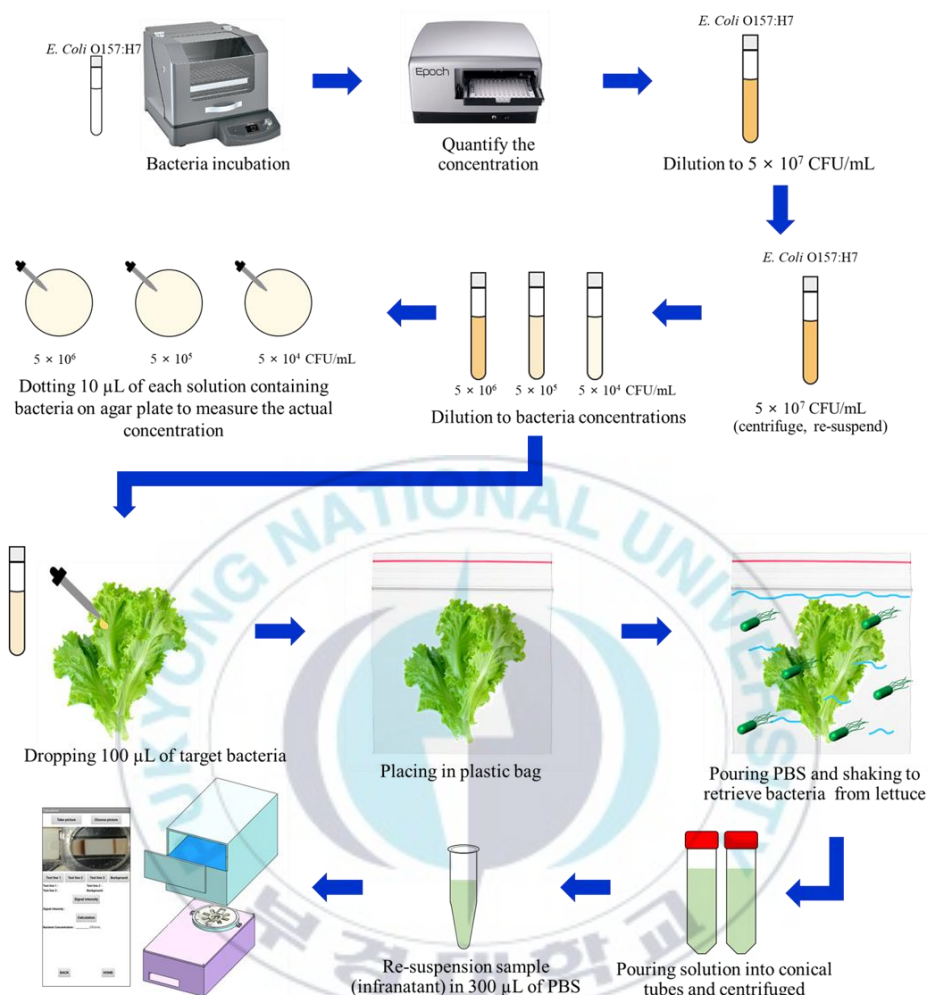
Figure 24. Schematics of each step of performing the detection of Bacteria from Contaminated Lettuce

3.8 Sensor Stability

The NC membrane was immobilized by goat anti-rabbit IgG with trehalose, and mouse *E. coli* O157 antibody with trehalose on the control line and the test line, respectively. The NC membrane was allowed to dry and keep at 4℃ with foil to prevent the light. In this study, we used the NC membrane with immobilize antibodies for 0 (immediately), 5, and 10 days to perform automated multistep LFIA with the *E. coli* O157:H7 as the bacteria target.

4. RESULT AND DISCUSSION

This chapter describes the result and discussion of our experiments in this study consisting of Calibration Curve using Smartphone Application, Detection Specificity, Sensor Stability, and Detection of Bacteria from Contaminated Lettuce.

4.1 Calibration Curve using Smartphone Application

The smartphone application's function was used to make the calibration curve that is used to determine the concentration of an unknown sample, and to calculate the limit of detection. In this study the *E. coli* O157:H7 samples whose concentrations ranged from 5×10^0 to 5×10^7 CFU/mL were used as the target bacteria sample for making a calibration curve. The signal intensity of each bacterial concentration was calculated from the smartphone application.

The result of the quantified signal intensity concerning the bacterial concentration is shown in **Figure 19**. The results of the signal intensity were calculated on the first page of the Calibration function of the smartphone and are used for making the calibration curve in **Figure 20**. The curve was fit among the data points within the linear range, in our study used the concentrations ranged between 5×10^3 to 5×10^7 CFU/mL. **Figure 25a**, shows the picture of the NC strip from the rotary pad taken by the camera function of the application. On the NC strip, it is apparent that the signal intensity begins to increase at a bacterial concentration of 5×10^4 CFU/mL. When compared the bacteria concentration ranged between 5×10^1 to 5×10^3 CFU/mL with the negative control, the signal intensity that appeared were close. Thus, based on this result, the LOD of the device by the naked eye is determined to be 5×10^4 CFU/mL. Additionally, by using the smartphone application and a formula 3.3 × standard deviation / slope, the LOD is calculated to be $5 \times 10^{1.3}$ CFU/mL (approximately 100 CFU/mL).

36
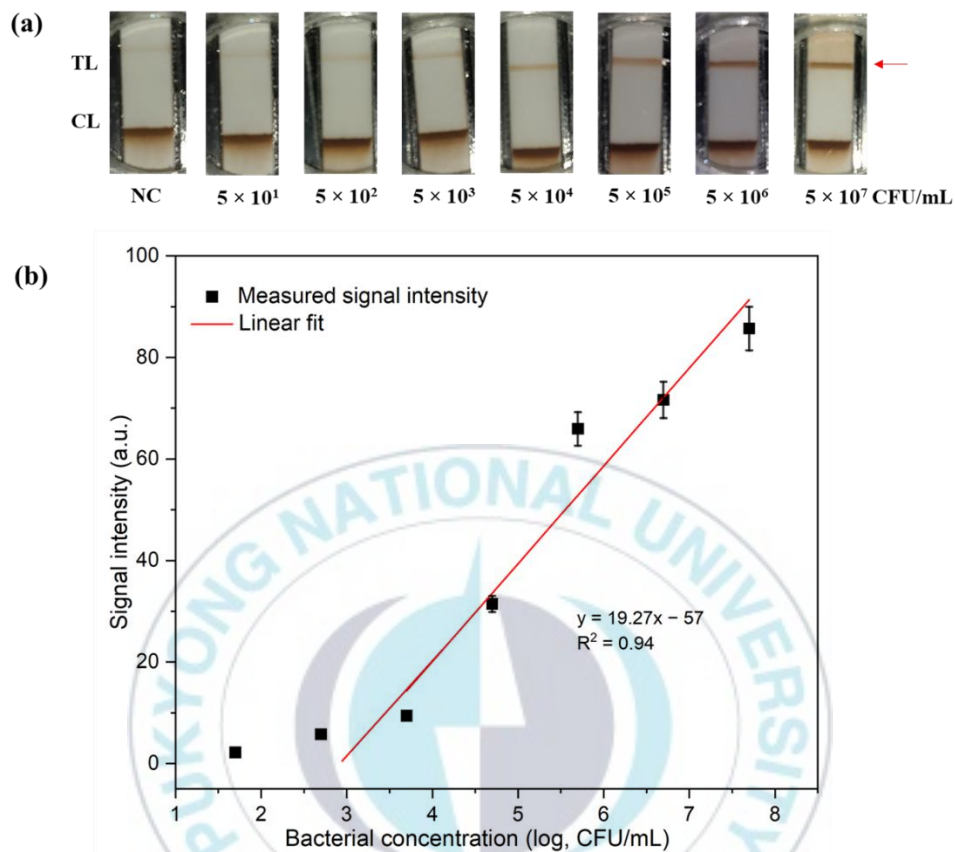
Figure 25. (a) Photos showing the signal generation on the NC strip of bacteria concentration 5×10^0 to 5×10^7 CFU/mL. TL and CL are the test line and control line, respectively. The red arrow indicates the location of signal on the test line. (b) Graph showing the calibration curve and the linear fit that was redrawn by the OriginLab software.

The calibration curve made by our application was redrawn using the OriginLab software to clearly represent is shown as **Figure 25b**. **Figure 25b** shows the sensitivity of the sensor or the slope of the linear range (red line) of the calibration curve that was calculated to be 19.27 intensity (a.u) / (5×10^1 CFU/mL). The condition of the experiment, such as flow duration, antibodies, enzymes, and substrates that the users use for the experiment will result in different calibration graphs. It is important to note that the calibration curve depends on each experiment condition. Thus, before performing the bacteria target detection in an unknown

sample, the users should make their own calibration curve. The equation of the calibration curve will be used to calculate in the experiment of bacteria target detection in an unknown sample.

4.2 Detection Specificity

To observe the specificity of the device that has the ability to detect specific bacteria; this study focuses on *E. coli* O157:H7 for detection. Two different genera of bacteria (*S. aureus* and *S.* Typhimurium) were used. **Figure 26** shows their detection results on the NC strip. The result shows a significant difference between the signal intensity when detecting different bacteria of the same concentration which was compared by making the comparison bar graph as shown in **Figure 27**. when loading *S. aureus* and *S.* Typhimurium in the NC membrane that had the antibodies for *E. coli* O157:H7 immobilized, a weak signal appears on the NC membrane. **Figure 26** and **Figure 2**7 clearly show that the signal intensity that detects *E. coli* O157:H7 is strong, and the detection of signal intensity of *S. aureus* and *S.* Typhimurium remained closed to the signal intensity of the negative control. This indicates that the detection can be performed with high specificity due to the specificity of the antibody used in this experiment.
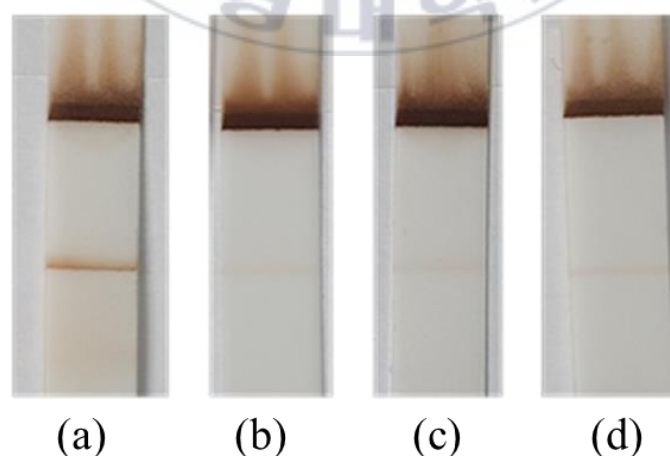
Figure 26. Photos of the detection result of different bacteria; (a) *E. coli* O157:H7, (b) *S. aureus*, (c) *S.* Typhimurium, and (d) Nagative contol.
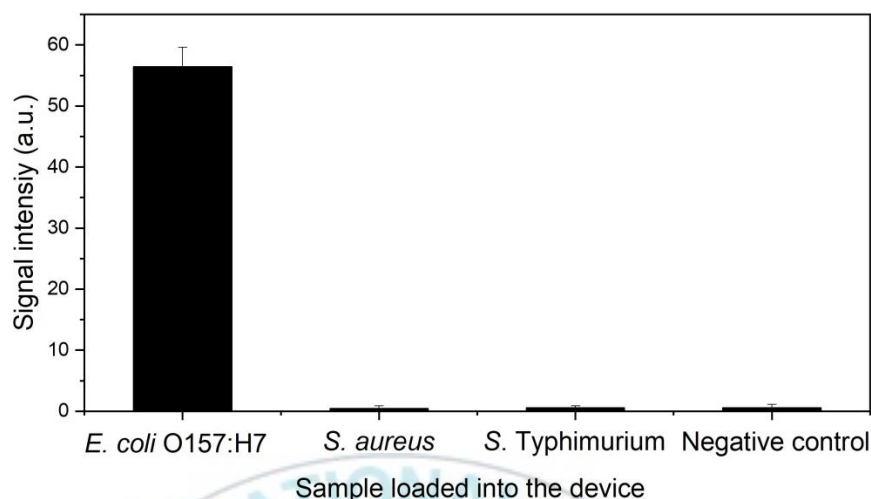
Figure 27. The bar graph of the detection intensity.

4.3 Sensor Stability

The stability test refers to the ability of reagent to retain its original performance and properties over a period of time when stored under defined conditions. This study demonstrate the stability test of the immobilized antibodies that performing the detection of the same concentration of *E. coli* O157:H7 bacteria, which concentration of *E. coli* O157:H7 is 5×10^7 CFU/mL. In the same experimental conditions, we have done the experiment immediately after immobilizing antibodies onto the NC membrane at a room temperature, and 5 and 10 days after the immobilization. The NC membrane that is immobilized for 5 and 10 days was store in 4°C.

The results of detecting bacteria target on the NC membrane immediately, 5, and 10 days of storage are shown in **Figure 28a–c**, respectively. With the naked eye, the results are not significantly different. The test line of the NC membrane calculated the quantified signal intensity using our application in the Calculation function. In addition, although looking with the naked eye will not be able to see a clear difference, our application can detect a little difference in the signal intensity of the test line of the NC membrane immediately, 5, and 10 days of storage is shown in

Table 3. However, the result is shown in **Figure 29**, which indicates that there is no statistically significant difference between the detection results for at least 10 days. The result of the stability test indicates that the antibodies used in our study can capture bacteria.

(a)   (b)   (c)
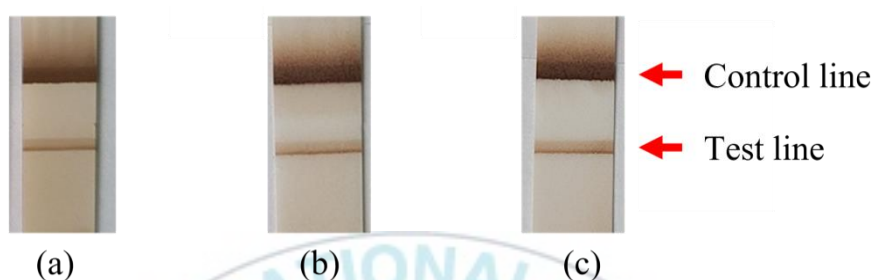
Figure 28. Result of detecting 5×10^7 CFU/mL *E. coli* O157:H7 on the NC membrane (a) immediately after immobilizing antibodies, (b) 5 days after, and (c) 10 days after immobilization.
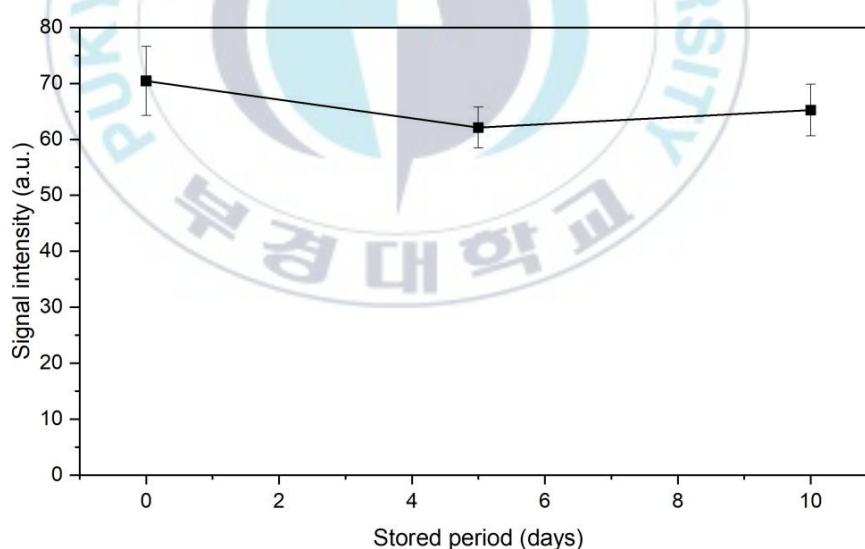
Figure 29. Graph that showing the quantified signal intensity of the test line obtained from the stability.

Table 3. The quantified signal intensity of the test line obtained from the stability.

Stored period (days)	Average of signal intensity (a.u.)	Standard deviation (stdev)
0 (immediately after immobilizing antibodies)	88.97	6.17
5	72.98	3.62
10	79.00	4.59

4.4 Detection of Bacteria from Contaminated Lettuce

The experiment of the detection of bacteria from contaminated lettuce was done to support that our device can actually be used to detect bacteria from contaminated fresh vegetables. The bacteria target concentrations ranging from 5×10^4 to 5×10^6 CFU/mL were used in this experiment, based on the calibration curve (the linear range) and the limit of detection. The portions of the target bacteria sample were dotted on an agar plate that contained a growth medium solidified with agar for inoculation, in which each concentration was repeated 3 times to check the accuracy of the experiment. The target bacteria samples were incubated overnight to determine the number of inoculated bacteria in the lettuce via Colony Counting. Additionally, the bacteria target sample that was retrieved from the lettuce was diluted to the bacteria target concentrations ranging from 5×10^4 to 5×10^6 CFU/mL and then were loaded into the rotary device the was performed the multistep immunoassay (the Automated Multistep LFIA) with the same condition with the experiment of making the calibration curve and analyzed using our smartphone application.

Table 4 shows the comparison of the number of bacteria inoculated to the lettuce that was calculated via Colony Counting (CFU/10 g), and the number of bacteria from the contaminated lettuce detected using LFIA (CFU/10 g), which the calculated concentration obtained from the smartphone application was combined with the re-suspension volume, inoculation volume, and dilution factor to calculate the number of bacteria retrieved from the lettuce in CFU/10g.

The results in **Table 4** indicate that the calculated concentration from the smartphone application is similar to the number of bacteria calculated via Colony

41

Counting. In trial 1, the target sample concentration at 5×10^4 CFU/mL, also the target sample concentrations of 5×10^5 and 5×10^6 CFU/mL of trial 2 show the calculated concentration from the smartphone application is higher than the calculated via Colony Counting. This can be mentioned that there are some mistakes such as the area that was chosen as the test line because the intensity can be changed when the chosen area was changed. However, most of the results are indicating that the calculated via Colony Counting is higher than the calculated concentration from the smartphone application. The reason for this case is there can be some bacteria loss during the retrieval process when collecting bacteria from the contaminated lettuce, which can contribute to the discrepancy between the amounts of inoculated bacteria and the number of the detected bacteria using LFIA.

Table 4. Comparison between the number of bacteria inoculated from counting colonies and the number of bacteria inoculated from the device performing multistep immunoassay on a lateral flow strip.

Trial	Number of Bacteria Inoculated to the Lettuce, calculated via Colony Counting (CFU/10 g)	Number of Bacteria from the Contaminated Lettuce Detected using LFIA (CFU/10 g)
1	2.37×10^3	3.33×10^3
	2.66×10^4	2.51×10^4
	3.16×10^5	1.85×10^5
2	1.31×10^3	1.22×10^3
	1.73×10^4	1.98×10^4
	2.13×10^5	2.23×10^5
3	1.85×10^3	1.70×10^3
	2.92×10^4	1.33×10^4
	3.49×10^5	3.43×10^5

However, the results can be considered to be satisfactory when considering the fact that the order of the measured bacteria number (calculated via Colony Counting) and

the order of the calculated bacteria number (calculated concentration via the smartphone application) are the same for all cases.

5. CONCLUSIONS

In conclusion, we demonstrated the detection of bacteria on LFIA using a multistep immunoassay platform, which was adapted from a rotary handheld into an automated system. It is controlled and operated through a developed smartphone application. The operation of our automatic multistep immunoassay platform can be easily performed without the need for specialists. It also takes only 30 minutes to complete, is inexpensive, requires one-time pipetting, and most importantly is automation that makes it not difficult to experiment. The principle of the automatic device is to use Bluetooth to connect from a smartphone application to the device that we design. The device has two main components: an electronic part that connects the automatic device to a smartphone, and a rotary part that is an essential part of detecting bacteria because it is the part that performs the Automated Multistep LFIA. The electronic part is divided into two parts: an electronic box that is used to put electronic devices and a cover box that is important to control and prevent the variation in the ambient light from the external environment when using the smartphone's camera to image the LFA strip. The rotary device is designed with 8 compartments for absorbent pads and sample pads, and the NC membrane to display the result of bacterial detection. For applications, it has three functions: Setting and Run, Calibration, and Calculation, all of which are easy to use and convenient to connect to the device as well as analysis. The detection results of E. coli O157:H7 bacteria from performing automated Multistep LFIA of our automatic rotary device and smartphone application are highly accurate and specific. The limit of detection of our device is $5 \times 10^{1.3}$ CFU/mL (approximately 100 CFU/mL) follow the calibration curve. We also present that the reagents that we used for detecting this target bacteria are specific to detection. In addition, our designed device satisfactorily detects bacteria from fresh vegetables. The above can indicate that the developed app and device are designed to support the automation of multistep assays requiring multiple

pipetting and incubation steps and to assist untrained personnel in detecting point-of-care needs.

Currently, our device was designed only for a specific smartphone (our smartphone) which means the size, and length of the device including a jig inside the cover box was used for our smartphone. The plate (smartphone holder) that has a jig was attached to the cover box and has important for positioning the smartphone. To improve the device can use with other smartphones, this part should be fixed to be compatible for other smartphones such as making the plates for the other smartphone and design the cover box to have the ability to change the plate. Furthermore, we always prepare the sample pad and add the reagents for each step before performing the bacteria detection. In the future, the added reagent in the sample pad (HRP-conjugate antibody and DAB) should be developed to long-term dry stored. This will reduce the time to adding the reagent.
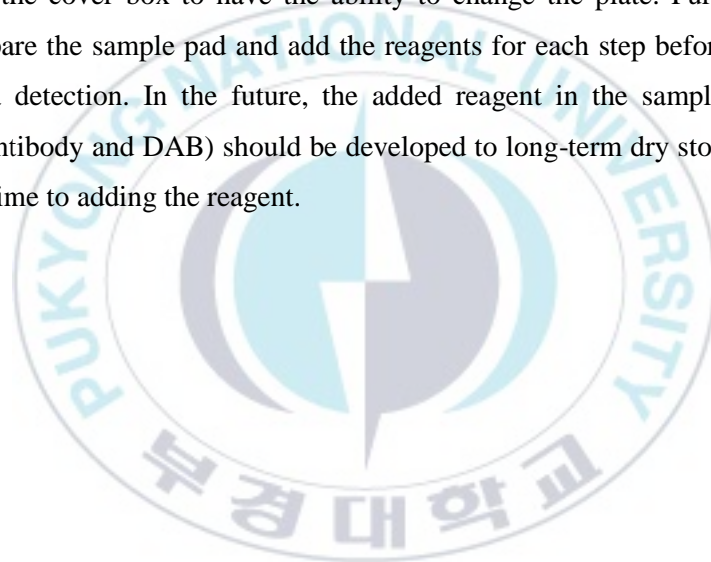
6. REFERENCES

[1]   W. H. Organization, *WHO estimates of the global burden of foodborne diseases: foodborne disease burden epidemiology reference group 2007-2015*. World Health Organization, 2015.

[2]   L. M. Zanin, D. T. da Cunha, V. V. de Rosso, V. D. Capriles, and E. Stedefeldt, "Knowledge, attitudes and practices of food handlers in food safety: An integrative review," *Food Research International,* vol. 100, pp. 53-62, 2017/10/01/ 2017, doi: https://doi.org/10.1016/j.foodres.2017.07.042.

[3]   C. D. o. P. Health. "FOODBORNE ILLNESSES AND OUTBREAKS." CDPH. https://www.cdph.ca.gov/Programs/CID/DCDC/Pages/FoodborneDiseasesan dOutbreaks.aspx (accessed 29 November 2022.

[4]   J. J. Kim, S. Ryu, and H. Lee, "Foodborne Illness Outbreaks in Gyeonggi Province, Korea, Following Seafood Consumption Potentially Caused by Kudoa septempunctata between 2015 and 2016," (in eng), *Osong Public Health Res Perspect,* vol. 9, no. 2, pp. 66-72, Apr 2018, doi: 10.24171/j.phrp.2018.9.2.05.

[5]   P. Padungtod, M. Kadohira, and G. Hill, "Livestock Production and Foodborne Diseases from Food Animals in Thailand," *Journal of Veterinary Medical Science,* vol. 70, no. 9, pp. 873-879, 2008, doi: 10.1292/jvms.70.873.

[6]   WHO. "Food safety." World Health Organization. https://www.who.int/news-room/fact-sheets/detail/food-safety (accessed 26 October, 2022).

[7]   A. A. Sher, M. A. Ashraf, B. E. Mustafa, and M. M. Raza, "Epidemiological trends of foodborne Campylobacter outbreaks in the United States of America, 1998–2016," *Food Microbiology,* vol. 97, p. 103751, 2021/08/01/ 2021, doi: https://doi.org/10.1016/j.fm.2021.103751.

[8]   S. SIVAPALASINGAM, C. R. FRIEDMAN, L. COHEN, and R. V. TAUXE, "Fresh Produce: A Growing Cause of Outbreaks of Foodborne Illness in the United States, 1973 through 1997," *Journal of Food Protection,* vol. 67, no. 10, pp. 2342-2353, 2004, doi: 10.4315/0362-028x-67.10.2342.

[9]   G. K. KOZAK, D. MacDONALD, L. LANDRY, and J. M. FARBER, "Foodborne Outbreaks in Canada Linked to Produce: 2001 through 2009," *Journal of Food Protection,* vol. 76, no. 1, pp. 173-183, 2013, doi: 10.4315/0362-028x.Jfp-12-126.

[10]   D. Michlmayr *et al.*, "Incubation Period, Spore Shedding Duration, and Symptoms of Enterocytozoon bieneusi Genotype C Infection in a Foodborne Outbreak in Denmark, 2020," *Clinical Infectious Diseases,* vol. 75, no. 3, pp. 468-475, 2022, doi: 10.1093/cid/ciab949.

[11]   E. Cherchame *et al.*, "Salmonella enterica subsp. enterica Welikade: guideline for phylogenetic analysis of serovars rarely involved in foodborne outbreaks," *BMC Genomics,* vol. 23, no. 1, p. 217, 2022/03/19 2022, doi: 10.1186/s12864-022-08439-2.

[12]   S. H. Lee, J. W. Yun, J. H. Lee, Y. H. Jung, and D. H. Lee, "Trends in recent waterborne and foodborne disease outbreaks in South Korea, 2015-2019," (in eng), *Osong Public Health Res Perspect,* vol. 12, no. 2, pp. 73-79, Apr 2021, doi: 10.24171/j.phrp.2021.12.2.04.

[13]   R. M. Callejón, M. I. Rodríguez-Naranjo, C. Ubeda, R. Hornedo-Ortega, M. C. Garcia-Parrilla, and A. M. Troncoso, "Reported foodborne outbreaks due to fresh produce in the United States and European Union: trends and causes," (in eng), *Foodborne Pathog Dis,* vol. 12, no. 1, pp. 32-8, Jan 2015, doi: 10.1089/fpd.2014.1821.

[14]   C. K. Carstens, J. K. Salazar, and C. Darkoh, "Multistate Outbreaks of Foodborne Illness in the United States Associated With Fresh Produce From 2010 to 2017," (in eng), *Front Microbiol,* vol. 10, p. 2667, 2019, doi: 10.3389/fmicb.2019.02667.

[15] A. E. White *et al.*, "Foodborne Illness Outbreaks Reported to National Surveillance, United States, 2009-2018," (in eng), *Emerg Infect Dis,* vol. 28, no. 6, pp. 1117-1127, Jun 2022, doi: 10.3201/eid2806.211555.

[16] D. F. Safety. "Foodborne illness: How do I prevent it?" Dairy Food Safety. https://www.dairysafe.vic.gov.au/consumers/keeping-dairy-food-safe/foodborne-illness-how-do-i-prevent-it (accessed 19 December 2022.

[17] V. García-Cañas, C. Simó, M. Herrero, E. Ibáñez, and A. Cifuentes, "Present and future challenges in food analysis: foodomics," (in eng), *Anal Chem,* vol. 84, no. 23, pp. 10150-9, Dec 4 2012, doi: 10.1021/ac301680q.

[18] R. L. Bell, K. G. Jarvis, A. R. Ottesen, M. A. McFarland, and E. W. Brown, "Recent and emerging innovations in Salmonella detection: a food and environmental perspective," *Microbial Biotechnology,* https://doi.org/10.1111/1751-7915.12359 vol. 9, no. 3, pp. 279-292, 2016/05/01 2016, doi: https://doi.org/10.1111/1751-7915.12359.

[19] J. H. Shin *et al.*, "Multiplexed Detection of Foodborne Pathogens from Contaminated Lettuces Using a Handheld Multistep Lateral Flow Assay Device," (in eng), *J Agric Food Chem,* vol. 66, no. 1, pp. 290-297, Jan 10 2018, doi: 10.1021/acs.jafc.7b03582.

[20] G. Xing, W. Zhang, N. Li, Q. Pu, and J.-M. Lin, "Recent progress on microfluidic biosensors for rapid detection of pathogenic bacteria," *Chinese Chemical Letters,* vol. 33, no. 4, pp. 1743-1751, 2022/04/01/ 2022, doi: https://doi.org/10.1016/j.cclet.2021.08.073.

[21] B. Priyanka, R. K. Patil, and S. Dwarakanath, "A review on detection methods used for foodborne pathogens," (in eng), *Indian J Med Res,* vol. 144, no. 3, pp. 327-338, Sep 2016, doi: 10.4103/0971-5916.198677.

[22] W. ADOPTED 20 MARCH , DC, NATIONAL ADVISORY COMMITTEE ON MICROBIOLOGICAL CRITERIA FOR FOODS, "Response to Questions Posed by the Food Safety and Inspection Service Regarding Determination of the Most Appropriate Technologies for the Food Safety and Inspection Service To

Adopt in Performing Routine and Baseline Microbiological Analyses†,‡," *Journal of Food Protection,* vol. 73, no. 6, pp. 1160-1200, 2010, doi: 10.4315/0362-028x-73.6.1160.

[23] A. K. Bhunia, "One day to one hour: how quickly can foodborne pathogens be detected?," *Future Microbiology,* vol. 9, no. 8, pp. 935-946, 2014, doi: 10.2217/fmb.14.61.

[24] A. C. G. Foddai and I. R. Grant, "Methods for detection of viable foodborne pathogens: current state-of-art and future prospects," (in eng), *Appl Microbiol Biotechnol,* vol. 104, no. 10, pp. 4281-4288, May 2020, doi: 10.1007/s00253-020-10542-x.

[25] F. J. Cousin, R. Le Guellec, V. Chuat, M. Dalmasso, J.-M. Laplace, and M. Cretenet, "Multiplex PCR for rapid identification of major lactic acid bacteria genera in cider and other fermented foods," *International Journal of Food Microbiology,* vol. 291, pp. 17-24, 2019/02/16/ 2019, doi: https://doi.org/10.1016/j.ijfoodmicro.2018.11.004.

[26] W. E. Hill, "The polymerase chain reaction: applications for the detection of foodborne pathogens," (in eng), *Crit Rev Food Sci Nutr,* vol. 36, no. 1-2, pp. 123-73, Jan 1996, doi: 10.1080/10408399609527721.

[27] J.-H. Kim, S. Jung, and S. W. Oh, "Combination of bacteria concentration and DNA concentration for rapid detection of E. coli O157:H7, L. monocytogenes, and S. Typhimurium without microbial enrichment," *LWT,* vol. 117, p. 108609, 09/01 2019, doi: 10.1016/j.lwt.2019.108609.

[28] J.-H. Kim and S.-W. Oh, "A colorimetric lateral flow assay based on multiplex PCR for the rapid detection of viable Escherichia coli O157:H7 and Salmonella Typhimurium without enrichment," *LWT,* vol. 152, p. 112242, 2021/12/01/ 2021, doi: https://doi.org/10.1016/j.lwt.2021.112242.

[29] O. Strohmeier, N. Marquart, D. Mark, G. Roth, R. Zengerle, and F. von Stetten, "Real-time PCR based detection of a panel of food-borne pathogens on a centrifugal microfluidic "LabDisk" with on-disk quality controls and

standards for quantification," *Analytical Methods,* 10.1039/C3AY41822G vol. 6, no. 7, pp. 2038-2046, 2014, doi: 10.1039/C3AY41822G.

[30]   R. Fung *et al.*, "Clams and potential foodborne Toxoplasma gondii in Nunavut, Canada," *Zoonoses and Public Health,* https://doi.org/10.1111/zph.12822 vol. 68, no. 3, pp. 277-283, 2021/05/01 2021, doi: https://doi.org/10.1111/zph.12822.

[31]   L. F. Lalonde, V. Xie, J. R. Oakley, and V. A. Lobanov, "Optimization and validation of a loop-mediated isothermal amplification (LAMP) assay for detection of Giardia duodenalis in leafy greens," (in eng), *Food Waterborne Parasitol,* vol. 23, p. e00123, Jun 2021, doi: 10.1016/j.fawpar.2021.e00123.

[32]   J. W. Lee, V. D. Nguyen, and T. S. Seo, "Paper-based Molecular Diagnostics for the Amplification and Detection of Pathogenic Bacteria from Human Whole Blood and Milk Without a Sample Preparation Step," *BioChip Journal,* vol. 13, no. 3, pp. 243-250, 2019/09/01 2019, doi: 10.1007/s13206-019-3310-8.

[33]   J. W.-F. Law, N.-S. Ab Mutalib, K.-G. Chan, and L.-H. Lee, "Rapid methods for the detection of foodborne bacterial pathogens: principles, applications, advantages and limitations," (in English), *Frontiers in Microbiology,* Review vol. 5, 2015-January-12 2015, doi: 10.3389/fmicb.2014.00770.

[34]   H. Liu, G. Hopping, U. Vaidyanathan, Y. Ronquillo, P. Hoopes, and M. Majid, "Polymerase Chain Reaction and Its Application in the Diagnosis of Infectious Keratitis," *Medical hypothesis, discovery & innovation ophthalmology journal,* vol. 8, pp. 152-155, 10/01 2019.

[35]   S. Gunasegar and V. K. Neela, "Evaluation of diagnostic accuracy of loop-mediated isothermal amplification method (LAMP) compared with polymerase chain reaction (PCR) for Leptospira spp. in clinical samples: a systematic review and meta-analysis," *Diagnostic Microbiology and Infectious Disease,* vol. 100, no. 3, p. 115369, 2021/07/01/ 2021, doi: https://doi.org/10.1016/j.diagmicrobio.2021.115369.

[36] D. Xu, L. Ji, X. Wu, W. Yan, and L. Chen, "Detection and differentiation of Vibrio parahaemolyticus by multiplexed real-time PCR," *Canadian Journal of Microbiology,* vol. 64, no. 11, pp. 809-815, 2018, doi: 10.1139/cjm-2018-0083 %M 29864373.

[37] P. A. Kokkinos, P. G. Ziros, M. Bellou, and A. Vantarakis, "Loop-Mediated Isothermal Amplification (LAMP) for the Detection of Salmonella in Food," *Food Analytical Methods,* vol. 7, no. 2, pp. 512-526, 2014/02/01 2014, doi: 10.1007/s12161-013-9748-8.

[38] C. Ponce *et al.*, "Diagnostic accuracy of loop-mediated isothermal amplification (LAMP) for screening patients with imported malaria in a non-endemic setting," (in eng), *Parasite,* vol. 24, p. 53, 2017, doi: 10.1051/parasite/2017054. Précision diagnostique de l'amplification isothermique d'ADN en boucle (LAMP) pour le dépistage des patients avec paludisme importé dans un contexte non endémique.

[39] X. Zhao, C. W. Lin, J. Wang, and D. H. Oh, "Advances in rapid detection methods for foodborne pathogens," (in eng), *J Microbiol Biotechnol,* vol. 24, no. 3, pp. 297-312, Mar 28 2014, doi: 10.4014/jmb.1310.10013.

[40] S.-Y. Wu, J. Hulme, and S. S. A. An, "Recent trends in the detection of pathogenic Escherichia coli O157 : H7," *BioChip Journal,* vol. 9, no. 3, pp. 173-181, 2015/09/01 2015, doi: 10.1007/s13206-015-9208-9.

[41] J. Fung, S. K. P. Lau, and P. C. Y. Woo, "Antigen Capture Enzyme-Linked Immunosorbent Assay for Detecting Middle East Respiratory Syndrome Coronavirus in Humans," (in eng), *Methods Mol Biol,* vol. 2099, pp. 89-97, 2020, doi: 10.1007/978-1-0716-0211-9_7.

[42] L. Zhu, J. He, X. Cao, K. Huang, Y. Luo, and W. Xu, "Development of a double-antibody sandwich ELISA for rapid detection of Bacillus Cereus in food," *Scientific Reports,* vol. 6, no. 1, p. 16092, 2016/03/15 2016, doi: 10.1038/srep16092.

[43]   K. Gu *et al.*, "Development of nanobody-horseradish peroxidase-based sandwich ELISA to detect Salmonella Enteritidis in milk and in vivo colonization in chicken," *Journal of Nanobiotechnology,* vol. 20, no. 1, p. 167, 2022/03/31 2022, doi: 10.1186/s12951-022-01376-y.

[44]   M. S. Khan, T. Pande, and T. G. M. van de Ven, "Qualitative and quantitative detection of T7 bacteriophages using paper based sandwich ELISA," *Colloids and Surfaces B: Biointerfaces,* vol. 132, pp. 264-270, 2015/08/01/ 2015, doi: https://doi.org/10.1016/j.colsurfb.2015.05.028.

[45]   B. Pang *et al.*, "Development of a low-cost paper-based ELISA method for rapid Escherichia coli O157:H7 detection," (in eng), *Anal Biochem,* vol. 542, pp. 58-62, Feb 1 2018, doi: 10.1016/j.ab.2017.11.010.

[46]   Y. Zhao *et al.*, "Rapid and accurate detection of Escherichia coli O157:H7 in beef using microfluidic wax-printed paper-based ELISA," *Analyst,* 10.1039/D0AN00224K vol. 145, no. 8, pp. 3106-3115, 2020, doi: 10.1039/D0AN00224K.

[47]   S. Sakamoto *et al.*, "Enzyme-linked immunosorbent assay for the quantitative/qualitative analysis of plant secondary metabolites," (in eng), *J Nat Med,* vol. 72, no. 1, pp. 32-42, Jan 2018, doi: 10.1007/s11418-017-1144-z.

[48]   R. Pan *et al.*, "Gold nanoparticle-based enhanced lateral flow immunoassay for detection of Cronobacter sakazakii in powdered infant formula," (in eng), *J Dairy Sci,* vol. 101, no. 5, pp. 3835-3843, May 2018, doi: 10.3168/jds.2017-14265.

[49]   P. Wu *et al.*, "Multimodal capture – antibody-independent lateral flow immunoassay based on AuNF – PMBA for point-of-care diagnosis of bacterial urinary tract infections," *Chemical Engineering Journal,* vol. 451, p. 139021, 2023/01/01/ 2023, doi: https://doi.org/10.1016/j.cej.2022.139021.

[50]   C. Deng *et al.*, "An Emerging Fluorescent Carbon Nanobead Label Probe for Lateral Flow Assays and Highly Sensitive Screening of Foodborne Toxins and

Pathogenic Bacteria," *Analytical Chemistry,* vol. 94, no. 33, pp. 11514-11520, 2022/08/23 2022, doi: 10.1021/acs.analchem.2c01430.

[51]   C. Song, J. Liu, J. Li, and Q. Liu, "Dual FITC lateral flow immunoassay for sensitive detection of Escherichia coli O157:H7 in food samples," *Biosensors and Bioelectronics,* vol. 85, pp. 734-739, 2016/11/15/ 2016, doi: https://doi.org/10.1016/j.bios.2016.05.057.

[52]   A. H. A. Hassan, J. F. Bergua, E. Morales-Narváez, and A. Mekoçi, "Validity of a single antibody-based lateral flow immunoassay depending on graphene oxide for highly sensitive determination of E. coli O157:H7 in minced beef and river water," *Food Chemistry,* vol. 297, p. 124965, 2019/11/01/ 2019, doi: https://doi.org/10.1016/j.foodchem.2019.124965.

[53]   H.-S. Kim, H. Ko, M.-J. Kang, and J.-C. Pyun, "Highly sensitive rapid test with chemiluminescent signal bands," *BioChip Journal,* vol. 4, no. 2, pp. 155-160, 2010/06/01 2010, doi: 10.1007/s13206-010-4211-z.

[54]   S. Park, H. Kim, S. H. Paek, J. W. Hong, and Y. K. Kim, "Enzyme-linked immuno-strip biosensor to detect Escherichia coli O157:H7," (in eng), *Ultramicroscopy,* vol. 108, no. 10, pp. 1348-51, Sep 2008, doi: 10.1016/j.ultramic.2008.04.063.

[55]   J. H. Shin and J. K. Park, "Functional Packaging of Lateral Flow Strip Allows Simple Delivery of Multiple Reagents for Multistep Assays," (in eng), *Anal Chem,* vol. 88, no. 21, pp. 10374-10378, Nov 1 2016, doi: 10.1021/acs.analchem.6b02869.

[56]   Y.-D. Ma *et al.*, "A sample-to-answer, portable platform for rapid detection of pathogens with a smartphone interface," *Lab on a Chip,* 10.1039/C9LC00797K vol. 19, no. 22, pp. 3804-3814, 2019, doi: 10.1039/C9LC00797K.

[57]   T. Wang, S. Kim, and J. H. An, "A novel CMOS image sensor system for quantitative loop-mediated isothermal amplification assays to detect food-

borne pathogens," *Journal of Microbiological Methods,* vol. 133, pp. 1-7, 2017/02/01/ 2017, doi: https://doi.org/10.1016/j.mimet.2016.12.002.

[58] Y.-C. Wang *et al.*, "Turntable Paper-Based Device to Detect Escherichia coli," *Micromachines,* vol. 12, no. 2, p. 194, 2021. [Online]. Available: https://www.mdpi.com/2072-666X/12/2/194.

[59] C.-M. Shih *et al.*, "Paper-based ELISA to rapidly detect Escherichia coli," *Talanta,* vol. 145, pp. 2-5, 2015/12/01/ 2015, doi: https://doi.org/10.1016/j.talanta.2015.07.051.

[60] S. Banik *et al.*, "Recent trends in smartphone-based detection for biomedical applications: a review," *Analytical and Bioanalytical Chemistry,* vol. 413, no. 9, pp. 2389-2406, 2021/04/01 2021, doi: 10.1007/s00216-021-03184-z.

[61] W. Zhao, S. Tian, L. Huang, K. Liu, L. Dong, and J. Guo, "A smartphone-based biomedical sensory system," *Analyst,* 10.1039/C9AN02294E vol. 145, no. 8, pp. 2873-2891, 2020, doi: 10.1039/C9AN02294E.

[62] Y. Liu, A. M. Rollins, R. M. Levenson, F. Fereidouni, and M. W. Jenkins, "Pocket MUSE: an affordable, versatile and high-performance fluorescence microscope using a smartphone," *Communications Biology,* vol. 4, no. 1, p. 334, 2021/03/12 2021, doi: 10.1038/s42003-021-01860-5.

[63] M. K. Kanakasabapathy *et al.*, "Rapid, label-free CD4 testing using a smartphone compatible device," *Lab on a Chip,* 10.1039/C7LC00273D vol. 17, no. 17, pp. 2910-2919, 2017, doi: 10.1039/C7LC00273D.

[64] H. Yu *et al.*, "Malaria Screener: a smartphone application for automated malaria screening," *BMC Infectious Diseases,* vol. 20, no. 1, p. 825, 2020/11/11 2020, doi: 10.1186/s12879-020-05453-1.

[65] S. Lee, G. Kim, and J. Moon, "Performance Improvement of the One-Dot Lateral Flow Immunoassay for Aflatoxin B1 by Using a Smartphone-Based Reading System," *Sensors,* vol. 13, no. 4, pp. 5109-5116, 2013. [Online]. Available: https://www.mdpi.com/1424-8220/13/4/5109.

[66]   Z. Liu *et al.*, "A smartphone-based dual detection mode device integrated with two lateral flow immunoassays for multiplex mycotoxins in cereals," *Biosensors and Bioelectronics,* vol. 158, p. 112178, 2020/06/15/ 2020, doi: https://doi.org/10.1016/j.bios.2020.112178.

[67]   Y. Jung, Y. Heo, J. J. Lee, A. Deering, and E. Bae, "Smartphone-based lateral flow imaging system for detection of food-borne bacteria E.coli O157:H7," *Journal of Microbiological Methods,* vol. 168, p. 105800, 2020/01/01/ 2020, doi: https://doi.org/10.1016/j.mimet.2019.105800.

[68]   B. Jin *et al.*, "Lateral flow aptamer assay integrated smartphone-based portable device for simultaneous detection of multiple targets using upconversion nanoparticles," *Sensors and Actuators B: Chemical,* vol. 276, pp.   48-56,   2018/12/10/   2018,   doi: https://doi.org/10.1016/j.snb.2018.08.074.

[69]   E. Trofimchuk, A. Nilghaz, S. Sun, and X. Lu, "Determination of norfloxacin residues in foods by exploiting the coffee-ring effect and paper-based microfluidics device coupling with smartphone-based detection," *Journal of Food Science,* vol. 85, no. 3, pp. 736-743, 2020, doi: https://doi.org/10.1111/1750-3841.15039.

[70]   S.-M. Yang, S. Lv, W. Zhang, and Y. Cui, "Microfluidic Point-of-Care (POC) Devices in Early Diagnosis: A Review of Opportunities and Challenges," *Sensors,* vol. 22, no. 4, p. 1620, 2022. [Online]. Available: https://www.mdpi.com/1424-8220/22/4/1620.

[71]   S. H. Baek, C. Park, J. Jeon, and S. Park, "Three-Dimensional Paper-Based Microfluidic Analysis Device for Simultaneous Detection of Multiple Biomarkers with a Smartphone," *Biosensors,* vol. 10, no. 11, p. 187, 2020. [Online]. Available: https://www.mdpi.com/2079-6374/10/11/187.

[72]   A. K. Yetisen *et al.*, "Paper-based microfluidic system for tear electrolyte analysis," *Lab on a Chip,* 10.1039/C6LC01450J vol. 17, no. 6, pp. 1137-1148, 2017, doi: 10.1039/C6LC01450J.

[73]   Q. Wei *et al.*, "Detection and Spatial Mapping of Mercury Contamination in Water Samples Using a Smart-Phone," *ACS Nano,* vol. 8, no. 2, pp. 1121-1129, 2014/02/25 2014, doi: 10.1021/nn406571t.

[74]   V. Oncescu, D. O'Dell, and D. Erickson, "Smartphone based health accessory for colorimetric detection of biomarkers in sweat and saliva," *Lab on a Chip,* 10.1039/C3LC50431J vol. 13, no. 16, pp. 3232-3238, 2013, doi: 10.1039/C3LC50431J.

[75]   N. Lopez-Ruiz *et al.*, "Smartphone-Based Simultaneous pH and Nitrite Colorimetric Determination for Paper Microfluidic Devices," *Analytical Chemistry,* vol. 86, no. 19, pp. 9554-9562, 2014/10/07 2014, doi: 10.1021/ac5019205.

[76]   N. Cheng *et al.*, "Nanozyme-Mediated Dual Immunoassay Integrated with Smartphone for Use in Simultaneous Detection of Pathogens," *ACS Applied Materials & Interfaces,* vol. 9, no. 46, pp. 40671-40680, 2017/11/22 2017, doi: 10.1021/acsami.7b12734.

[77]   W. Chen *et al.*, "Mobile Platform for Multiplexed Detection and Differentiation of Disease-Specific Nucleic Acid Sequences, Using Microfluidic Loop-Mediated Isothermal Amplification and Smartphone Detection," *Analytical Chemistry,* vol. 89, no. 21, pp. 11219-11226, 2017/11/07 2017, doi: 10.1021/acs.analchem.7b02478.

[78]   S.-J. Yeo *et al.*, "Smartphone-Based Fluorescent Diagnostic System for Highly Pathogenic H5N1 Viruses," *Theranostics,* Research Paper vol. 6, no. 2, pp. 231-242, 2016, doi: 10.7150/thno.14023.

[79]   J. Fang *et al.*, "A sensing smartphone and its portable accessory for on-site rapid biochemical detection of marine toxins," *Analytical Methods,* 10.1039/C6AY01384H vol. 8, no. 38, pp. 6895-6902, 2016, doi: 10.1039/C6AY01384H.

[80]   E. W. Patton, M. Tissenbaum, and F. Harunani, "MIT App Inventor: Objectives, Design, and Development," in *Computational Thinking*

Education, S.-C. Kong and H. Abelson Eds. Singapore: Springer Singapore, 2019, pp. 31-49.

[81]   R. University of Nevada. "Lateral flow immunoassay." University of Nevada, Reno.   https://med.unr.edu/ddl/technology/lateral-flow-immunoassay (accessed 7 February, 2023).

[82]   K. M. Koczula and A. Gallotta, "Lateral flow assays," (in eng), *Essays Biochem,* vol. 60, no. 1, pp. 111-20, Jun 30 2016, doi: 10.1042/ebc20150012.

[83]   A.-C. Mirica, D. Stan, I.-C. Chelcea, C. M. Mihailescu, A. Ofiteru, and L.-A. Bocancia-Mateescu, "Latest Trends in Lateral Flow Immunoassay (LFIA) Detection Labels and Conjugation Process," (in English), *Frontiers in Bioengineering and Biotechnology,* Review vol. 10, 2022-June-14 2022, doi: 10.3389/fbioe.2022.922772.

[84]   D. Calabria *et al.*, "Recent Advancements in Enzyme-Based Lateral Flow Immunoassays," *Sensors,* vol. 21, no. 10, p. 3358, 2021. [Online]. Available: https://www.mdpi.com/1424-8220/21/10/3358.

[85]   S. Sachdeva, R. W. Davis, and A. K. Saha, "Microfluidic Point-of-Care Testing: Commercial Landscape and Future Directions," (in English), *Frontiers in Bioengineering and Biotechnology,* Review vol. 8, 2021-January-15 2021, doi: 10.3389/fbioe.2020.602659.

[86]   C. D.-F. F. Analysis. "Lateral Flow Immunoassay." Creative Diagnostics - Food & Feed Analysis. https://www.creative-diagnostics.com/food-analysis/tag-lateral-flow-immunoassay-30.htm (accessed 8 February, 2023).

[87]   JOYSBIO. "Lateral Flow Assays and Applications." JOYSBIO. https://en.joysbio.com/lateral-flow-assays-and-applications/ (accessed 9 February, 2023).

[88]   W. W.-W. Hsiao *et al.*, "Recent Advances in Novel Lateral Flow Technologies for Detection of COVID-19," *Biosensors,* vol. 11, no. 9, p. 295, 2021. [Online]. Available: https://www.mdpi.com/2079-6374/11/9/295.

[89] Cytiva. "Sandwich or competitive format: which is right for your LFA?" Cytiva. https://www.cytivalifesciences.com/en/us/news-center/lateral-flow-assay-format-sandwich-or-competitive-10001 (accessed 10 February, 2023).

[90] M. Majdinasab, M. Badea, and J. L. Marty, "Aptamer-Based Lateral Flow Assays: Current Trends in Clinical Diagnostic Rapid Tests," *Pharmaceuticals,* vol. 15, no. 1, p. 90, 2022. [Online]. Available: https://www.mdpi.com/1424-8247/15/1/90.

[91] E. B. Bahadır and M. K. Sezgintürk, "Lateral flow assays: Principles, designs and labels," *TrAC Trends in Analytical Chemistry,* vol. 82, pp. 286-306, 2016/09/01/ 2016, doi: https://doi.org/10.1016/j.trac.2016.06.006.

[92] W. S. Garrett and I. Mellman, "CHAPTER 16 - Studies of endocytosis," in *Dendritic Cells (Second Edition)*, M. T. Lotze and A. W. Thomson Eds. London: Academic Press, 2001, pp. 213-cp1.

[93] S. Hu, Q. Lu, and Y. Xu, "CHAPTER 17 - Biosensors based on direct electron transfer of protein," in *Electrochemical Sensors, Biosensors and their Biomedical Applications*, X. Zhang, H. Ju, and J. Wang Eds. San Diego: Academic Press, 2008, pp. 531-581.

[94] G. B. Wisdom, "Horseradish Peroxidase Labeling of IgG Antibody," in *The Protein Protocols Handbook*, J. M. Walker Ed. Totowa, NJ: Humana Press, 2009, pp. 681-683.

[95] A. M. Azevedo, V. C. Martins, D. M. F. Prazeres, V. Vojinović, J. M. S. Cabral, and L. P. Fonseca, "Horseradish peroxidase: a valuable tool in biotechnology," in *Biotechnology Annual Review*, vol. 9: Elsevier, 2003, pp. 199-247.

[96] K. Luo, H.-Y. Kim, M.-H. Oh, and Y.-R. Kim, "Paper-based lateral flow strip assay for the detection of foodborne pathogens: principles, applications, technological challenges and opportunities," *Critical Reviews in Food Science and Nutrition,* vol. 60, no. 1, pp. 157-170, 2020/01/02 2020, doi: 10.1080/10408398.2018.1516623.

[97] BIO-RAD. "HRP Substrate." BIO-RAD. https://www.bio-rad.com/featured/en/hrp-substrate.html (accessed 13 February, 2023).

[98] T. Scientific. "Anti-HRP Antibodies." ThernoFisher Scientific. https://www.thermofisher.com/kr/ko/home/life-science/antibodies/primary-antibodies/epitope-tag-antibodies/anti-hrp-antibodies.html (accessed 13 February, 2023).

[99] A. Kawde, X. Mao, H. Xu, Q. Zeng, Y. He, and G. Liu, "Moving Enzyme-Linked ImmunoSorbent Assay to the Point-of-Care Dry- Reagent Strip Biosensors," *American Journal of Biomedical Sciences,* pp. 23-32, 2010.

[100] C. Verlander, "Detection of horseradish peroxidase by colorimetry," *Nonisotopic DNA probe techniques,* pp. 185-201, 1992.

[101] C. Zhang, Y. Zhang, and S. Wang, "Development of Multianalyte Flow-through and Lateral-Flow Assays Using Gold Particles and Horseradish Peroxidase as Tracers for the Rapid Determination of Carbaryl and Endosulfan in Agricultural Products," *Journal of Agricultural and Food Chemistry,* vol. 54, no. 7, pp. 2502-2507, 2006/04/01 2006, doi: 10.1021/jf0531407.

[102] G. T. Hermanson, "Chapter 22 - Enzyme Modification and Conjugation," in *Bioconjugate Techniques (Third Edition)*, G. T. Hermanson Ed. Boston: Academic Press, 2013, pp. 951-957.

[103] ChemicalBook. "Application of 3,3'-Diaminobenzidine (DAB)." ChemicalBook. https://www.chemicalbook.com/Article/Application-of-3-3-Diaminobenzidine-DAB-.htm (accessed 20 February, 2023).

[104] T. Takizawa and J. M. Robinson, "Chapter 3 - Correlative Fluorescence and Transmission Electron Microscopy in Tissues," in *Methods in Cell Biology*, vol. 111, T. Müller-Reichert and P. Verkade Eds.: Academic Press, 2012, pp. 37-57.

[105] S. Zhang, J. Yang, and J. Lin, "3,3′–diaminobenzidine (DAB)–H2O2–HRP voltammetric enzyme-linked immunoassay for the detection of

carcionembryonic antigen," *Bioelectrochemistry,* vol. 72, no. 1, pp. 47-52, 2008/02/01/ 2008, doi: https://doi.org/10.1016/j.bioelechem.2007.11.011.

ACKNOWLEDGEMENTS

PUBLICATIONS

International journal

<u>Pattarapon Phangwipas</u>, Balamurugan Thangavel, Joong Ho Shin, "Automated Multistep Lateral Flow Immunoassay Using a Smartphone for the Quantification of Foodborne Bacteria from Fresh Lettuce", Chemosensors (2023), 2 January 2023.